Extreme relativistic Compton scattering by *K*-shell electrons

Viorica Florescu[1,2] and Mihai Gavrila[2]
[1]*Department of Physics, University of Bucharest, MG11, Bucharest-Magurele 76900, Romania*
[2]*Institute for Theoretical Atomic, Molecular and Optical Physics, Harvard-Smithsonian Center for Astrophysics, Cambridge, Massachusetts 02138, USA*

(Received 14 July 2003; published 14 November 2003)

We have derived cross sections for Compton scattering of very hard incident photons ($\hbar\omega_1 \gg mc^2$) from *K*-shell electrons, exact in the nuclear charge *Z*. The nuclear potential was taken to be of Coulomb form. The calculation of the extreme relativistic (ER) *S*-matrix element involved was carried out analytically. In the present case, this is the viable alternative to an impracticable *ab initio* numerical computation. In order to obtain the dominant behavior of the matrix element in the large ω_1 limit, the momentum transferred to the nucleus needs to be ascribed a constant (albeit arbitrary) value in the limiting process. The result depends critically on the spectral range in which the scattered-photon energy ω_2 is situated. We start by considering the ω_2 range covering the Compton line, for which the ratio ω_2/ω_1 needs to be kept finite. We show that in the ER limit the Dirac electron spinors and Green's operator entering the *S*-matrix element can be replaced by their relativistically modified Schrödinger counterparts. This allows the application of integration methods developed by us earlier for the nonrelativistic matrix element. Remarkably enough, the sixfold integrals of the ER matrix element can eventually be reduced to single integrals, expressible in terms of generalized hypergeometric functions. The doubly differential cross section $d^2\sigma/d\omega_2\, d\Omega_2$ for the range of Compton line finally results as a twofold integration, requiring a simple numerical computation. This is a rather unique example of a most elaborate Coulomb problem that could be solved analytically, essentially in closed form. We subsequently consider the low- ($\omega_2 \to 0$) and high-frequency ($\omega_2 \to \omega_2^{\max}$) ends of the scattered photon spectrum. For $\omega_2 \to 0$ we find the expected infrared divergence, and verify the soft-photon theorem, which represents an important check on our calculation. Finally, we present our numerical results for $d^2\sigma/d\omega_2\, d\Omega_2$, analyzed at fixed ω_2 (angular distributions), or fixed photon scattering angle (spectral distributions). We discuss the "defect" and the width of the Compton line for both distributions.

DOI: 10.1103/PhysRevA.68.052709 PACS number(s): 32.80.Cy

I. INTRODUCTION

The binding of an atomic electron entering Compton scattering has the effect of broadening and shifting the spectral line of the scattered photon with respect to that of a free electron at rest. The effect depends critically on the energy of the initial photon. At x-ray energies ($\hbar\omega_1 \ll mc^2$), where only outer shell, weakly bound electrons contribute prominently to the scattering, the effect can be treated within nonrelativistic (NR) quantum theory. In this case, the profile of the Compton line provides valuable information on their momentum distribution in the initial state, a fact extensively studied theoretically and experimentally (e.g., see Refs. [1,2], and references therein). At higher, γ-ray energies, for which $\hbar\omega_1$ is no longer small with respect to mc^2, relativistic theory is needed for the description, both because of the high energy of the incident photons, and the high nuclear charges *Z* of the elements of practical interest (appreciable αZ). An overview of the relativistic regime of Compton scattering was recently presented by Bergstrom and Pratt [3], see also Ref. [4].

Relativity is hard to deal with, so that various approximations have been considered. A significant advancement was the "relativistic impulse approximation," e.g., see Ribberfors [5] and references therein. This heuristic approach is quite successful in describing the Compton line at higher energies, but can give no information on special features of the spectrum, such as the infrared divergence or the resonant Raman-Compton structures. It does have the advantage of requiring a modest amount of computation. Whereas, there exists an *a priori* justification for the validity of the NR impulse approximation, none has been given so far for its relativistic version.

The definitive approach for solving the Compton problem within the independent-electron approximation is the integration of its relativistic *S*-matrix element in the Furry picture of QED (for the theoretical background of the relativistic treatment, see Akhiezer and Berestetskii, Sec. 35 of Ref. [6]). In general, the evaluation has to be done numerically. Eventually, the "numerical *S*-matrix approach" was achieved in the pivotal work by Suric, Bergstrom, Pisk, and Pratt [7]. Their program is capable of handling all atomic shells, within the independent-electron approximation with a relativistic central potential of the Hartree-Fock-Slater type. It offers a unified treatment of the whole photon spectrum, can achieve high numerical accuracy, and represents a trustworthy basis for the analysis of experimental data. It is limited, however, at high incoming photon energies $\hbar\omega_1$, by the convergence of the partial wave summation it contains. In practice, the limitation sets in at about $\hbar\omega_1 \simeq 2\, mc^2$.

The goal of our paper is to treat the extreme-relativistic (ER) case $\hbar\omega_1 \gg mc^2$ of Compton scattering, left uncovered by the numerical *S*-matrix approach. We shall derive analytic cross sections for the *K* shell, exact in *Z* to dominant order in $mc^2/\hbar\omega_1$. We are considering the case of a Coulomb potential, ignoring therefore screening corrections, which for the *K* shell are known to be small. We proceed from the *S*-matrix element for Compton scattering (Ref. [6], Sec. 35), our approximation being that of retaining systematically only the dominant order in $mc^2/\hbar\omega_1$. We shall focus mainly on the cross section $d^2\sigma/d\omega_2\, d\Omega_2$, differential with respect to the energy and angles of the scattered photon.

The method we use for integrating the ER matrix element is based on a combination of analytic procedures developed earlier in related contexts (NR Compton scattering [8], and ER Rayleigh scattering [9]). We shall show that the Dirac spinors and Green's operator needed in the calculation of the *extreme relativistic* Compton matrix element can be replaced by their *nonrelativistic* counterparts, taken with relativistically modified parameters. This allows the integration of the ER matrix element in a manner similar to the NR case [8]. The physical role of the many parameters of the scattering is explicitly displayed by the formulas. We have here a most elaborate Coulomb problem for which it was possible to complete the calculation analytically and obtain the result in closed form (hypergeometric functions), in a situation when a direct numerical computation is still prohibitive.

The problem we are treating was discussed, early on in the development of relativistic quantum mechanics, by Pauli and Heisenberg (see Ref. [10]), in connection with the behavior of the Compton line of an electron bound by a potential of nuclear charge *Z*, in the limit of very high energy $\hbar\omega_1 \gg mc^2$. The question posed was: does the cross section go over in this limit to the Klein-Nishina cross section for the free electron (independent of *Z*) or not? Using a qualitative argument based on the Klein-Nishina formula for a free electron with nonvanishing initial momentum, Pauli answered the question in negative [11]. On the occasion, he recognized that, in order to obtain the dominant behavior of the ER cross section, one needs to keep fixed the magnitude of the momentum transferred to the nucleus. An accompanying paper by Casimir [12] (also described in Sec. 35.3 of Ref. [6]), confirmed the existence of a *Z* dependence for the ER limit of the cross section. The approach used was inconsistent, however: in the evaluation of the exact *S*-matrix element, an exact expression was adopted for the initial *K*-shell Dirac spinor, whereas free electron approximations were used for the final state spinor and the Green's function. It has been later realized that such lowest order Born approximations do not lead to correct results, not even to lowest order in αZ, e.g., see Sec. VI of Ref. [13(a)]. Our answer to the Pauli-Heisenberg question will also be negative, but is the result of a consistent *S*-matrix approach.

Another theoretical question related to Compton scattering is that of the behavior of its *S*-matrix element and cross sections at low frequencies of the final photon ω_2 (designated as "soft"). Various studies have found these to be divergent for $\omega_2 \to 0$ (*infrared divergence*), in that they behave as $(1/\hbar\omega_2)$. The divergence is common to processes involving emission of a secondary photon that can share energy continuously with other particles (here the ejected electron), and is well known in QED (e.g., see Ref. [14]). Moreover, the matrix elements and cross sections for such processes are known to be related to those having the same initial condition, but no secondary photon, by "soft-photon theorems." For the Compton effect, the related process is the photoeffect, and the corresponding soft-photon theorem has been proven and discussed in various approximations by Gavrila, Sec. IV of Ref. [8] (exact nonrelativistic Coulomb case with retardation), McEnnan and Gavrila [13(a)] (relativistic Coulomb case, correct Born approximation), Bergstrom and Pratt [3] (numerical self-consistent potential case), and Rosenberg and Zhou [15] (exact nonrelativistic case with retardation, relativistic short range potential case). We shall check the theorem in the ER case. The related ER photoeffect cross sections for the *K* shell were derived by Boyer [16], Nagel [17], and Pratt [18]. This check offers an important confirmation of our analytic ER procedures. The issues concerning the infrared divergence and soft-photon theorem will only briefly be touched upon here, as they have been treated in more detail elsewhere [19,20].

Our endeavor on ER Compton scattering was encouraged by the new developments in the production of hard photons. Whereas there are few natural radioactive sources [21] that qualify for $\hbar\omega_1/mc^2 \gg 1$, remarkable advances have been made recently in the development of artificial sources, at electron storage ring facilities. Hard γ rays can be obtained by Compton backscattering of ultrarelativistic storage ring beams with intense optical photon beams. This can yield photons of MeV energy, depending on the velocity of the electrons and energy of the optical photons. A characteristic feature of these γ rays is that they are 100% linearly polarized. Energies of up to 32 MeV ($\hbar\omega/mc^2 \simeq 64$) have been reported [22(c)], 50 MeV are expected in the near future [22(a)], and up to 225 MeV are considered to be attainable. Such photons have a very large ratio $\hbar\omega/mc^2$, and would be excellent candidates for our cross sections.

However impressive the achievements of the laboratory sources may be at producing hard γ rays, they cannot compete with astrophysical sources. Spectacular progress of γ ray astronomy in the past decade has revealed the existence of sources emitting photons in the enormous energy span from 1 MeV to 10^7 MeV, in many cases with high fluxes, see Ref. [23]. The sources are either of galactic nature (e.g., spin-down pulsars, accreting x-ray binaries, supernovae remnants) or extragalactic (e.g., Seyfert and radio galaxies, blazars). This could represent another possible area of application of our formulas.

The content of the paper is the following. In Sec. II we present the relativistic matrix elements and cross sections of interest, within the Furry picture of QED. The incoming photons are taken to be linearly polarized, as are those produced by the storage-ring FEL sources. We consider mainly two cross sections: the quadruply differential cross section, in which both the characteristics of the scattered photon and ejected electron are recorded, and the doubly differential one, $d^2\sigma/d\omega_2\, d\Omega_2$, in which only the characteristics of the scattered photon are recorded. Section III discusses the ER kinematics. In defining the notion of ER limit, we show that the dominant order of the cross sections for $\omega_1 \to \infty$ is obtained by keeping the momentum transferred to the nucleus fixed in the limiting process. The result depends, however, critically on the value of ω_2. We consider the three ω_2 ranges: (i) soft-photon end ($\omega_2 \to 0$), (ii) Compton line (ω_2/ω_1 finite), and (iii) high-frequency end ($\omega_2 \to \omega_2^{\max}$), which require different treatments in the ER limit. In Secs. IV–VI we study the Compton line. Section IV introduces the quantities needed to calculate the matrix element in momentum space. Whereas the final state spinor and the Dirac Green's operator need to be expressed only to dominant order in $mc^2/\hbar\omega_1$, the initial state spinor has to be considered exactly, in order to ensure the exact Z dependence of the final results. Moreover, the final state spinor and the Dirac Green's operator can be expressed in terms of their nonrelativistic counterparts, with relativistically modified parameters. Thus, at start, the matrix element contains sixfold momentum integrals over nonrelativistic ingredients, and three parametric integrals. In Sec. V we outline the integration of the ER of the matrix element for the Compton line. The sixfold momentum space integrals can be evaluated in closed form, using formulas derived in our earlier works. Of the three parametric integrals, two can be carried out analytically, and the last one can be expressed in terms of hypergeometric functions of two variables, F_1. In Sec. VI we give the complete analytic expression of the doubly differential cross section $d^2\sigma/d\omega_2\, d\Omega_2$. This reduces to a single integral over the modulus square of a combination of F_1 functions. At zero photon-scattering angle, our results display a peculiar increase in order of magnitude of the cross section with respect to $(mc^2/\hbar\omega_1)$, no matter what the characteristics of the ejected electron are. For $Z\to 0$, the ER limit of the Klein-Nishina formula is regained. Section VII contains a brief presentation of the results for the low- and high-frequency ends of the scattered photon spectrum. At low frequencies ω_2, the ER form of the soft-photon theorem is obtained. At high frequencies (the "tip" of the spectrum), a peculiar increase in order of magnitude in $(mc^2/\hbar\omega_1)$ of the cross section is found. Section VIII contains our numerical results for $d^2\sigma/d\omega_2\, d\Omega_2$. We analyze the resulting angular distributions (at fixed ω_2) and spectral distributions (at fixed photon scattering angle). Both present a Compton peak, and we discuss the behavior of its "defect" (shift from free electron line) and width.

The calculations we present are tedious. We shall be giving in the following the minimum amount of analytic information needed to understand the physics, and to make possible the reproduction of the intermediate steps.

II. RELATIVISTIC MATRIX ELEMENTS AND CROSS SECTIONS

In the initial state of the process, we are dealing with a bound K-shell electron of energy $E_0 \equiv \gamma = (1-a^2)^{1/2}$ and magnetic quantum number $m_1 = \pm(1/2)$, plus a photon of momentum $\boldsymbol{\kappa}_1$, energy $\omega_1 \equiv \kappa_1$, and polarization vector $\mathbf{s}_1$. In the final state we have a continuum electron of asymptotic momentum $\mathbf{p}$, energy $E_p = (1+p^2)^{1/2}$, and magnetic quantum number $m_2 = \pm(1/2)$, the scattered photon having momentum $\boldsymbol{\kappa}_2$, energy $\omega_2 \equiv \kappa_2$, and polarization vector $\mathbf{s}_2$. We are using natural units ($\hbar = m = c = 1$), and denote $a \equiv \alpha Z$, where α is the fine-structure constant (in natural units $\alpha = e^2$).

The *quadruply differential cross section* for the Compton effect, in which all characteristics of the particles involved are recorded, can be written as [24]

$$d^4\sigma = \alpha^2 \frac{\kappa_2}{\kappa_1} |M^{(C)}|^2 \delta(E_0 + \kappa_1 - E_p - \kappa_2) \times p^2\, dp\, d\Omega_p\, d\kappa_2\, d\Omega_2, \tag{1}$$

where $d\Omega_2$ refers to the angles of $\boldsymbol{\kappa}_2$, and the δ function takes care of the conservation of energy

$$E_0 + \kappa_1 = E_p + \kappa_2. \tag{2}$$

The matrix element entering here is given by

$$M^{(C)} = M^{(1)} + M^{(2)}, \tag{3}$$

$$M^{(1)} = \int\int u_{\mathbf{p}m_2}^{(-)\dagger}(\mathbf{r}_2) e^{-i\boldsymbol{\kappa}_2\cdot\mathbf{r}_2} (\boldsymbol{\alpha}\cdot\mathbf{s}_2) G(\mathbf{r}_2,\mathbf{r}_1;\Omega_1) \times (\boldsymbol{\alpha}\cdot\mathbf{s}_1) e^{i\boldsymbol{\kappa}_1\cdot\mathbf{r}_1} u_{om_1}(\mathbf{r}_1)\, d\mathbf{r}_1 d\mathbf{r}_2, \tag{4}$$

$$M^{(2)} = \int\int u_{\mathbf{p}m_2}^{(-)\dagger}(\mathbf{r}_2) e^{i\boldsymbol{\kappa}_1\cdot\mathbf{r}_2} (\boldsymbol{\alpha}\cdot\mathbf{s}_1) G(\mathbf{r}_2,\mathbf{r}_1;\Omega_2) \times (\boldsymbol{\alpha}\cdot\mathbf{s}_2) e^{-i\boldsymbol{\kappa}_2\cdot\mathbf{r}_1} u_{om_1}(\mathbf{r}_1) d\mathbf{r}_1\, d\mathbf{r}_2. \tag{5}$$

$u_{om_1}(\mathbf{r}_1)$ is the initial spinor of the electron, and $u_{\mathbf{p}m_2}^{(-)}(\mathbf{r}_2)$ is the final, continuum spinor with incoming asymptotic spherical waves, normalized per momentum interval [25]. $G(\mathbf{r}_2,\mathbf{r}_1;\Omega)$ is the Green's function for the Dirac equation, with energy parameter Ω. Ω_1 and Ω_2 are given by

$$\Omega_1 = E_0 + \kappa_1 + i\epsilon, \quad \Omega_2 = E_0 - \kappa_2 - i\varepsilon. \tag{6}$$

The electron spinors and the Green's function satisfy the (homogeneous/inhomogeneous) Dirac equation

$$(\boldsymbol{\alpha}\cdot\mathbf{P} + \beta - a/r - \Omega)\Xi_D = YI. \tag{7}$$

For the electron spinors we need to take $\Xi_D \equiv u_{\mathbf{p}m}^{(-)}(\mathbf{r})$, $\Omega \equiv E$, $Y \equiv 0$, and for the Green's function $\Xi_D \equiv G(\mathbf{r},\mathbf{r}';\Omega), Y \equiv \delta(\mathbf{r}-\mathbf{r}')$; I is the 4×4 unit matrix.

In the following we shall not be interested in the dependence of the cross section on all the characteristics of the photons and electrons. We shall consider initially polarized photons but will not analyze their final polarizations. Neither shall we analyze the final polarizations of the electron. The corresponding quadruply differential cross section per K-shell electron is

$$d^4\tilde{\sigma} = \alpha^2 \frac{\kappa_2}{\kappa_1} \sum_{\mathbf{s}_2} \frac{1}{2} \sum_{m_1,m_2} |M^{(C)}|^2 \delta(E_0 + \kappa_1 - E_p - \kappa_2) \times p^2\, dp\, d\Omega_p\, d\kappa_2\, d\Omega_2. \tag{8}$$

Integration over the momenta of the electron gives the *doubly differential cross section*, we shall focus upon [26]

$$\frac{d^2\sigma}{d\kappa_2\,d\Omega_2}=\alpha^2\frac{\kappa_2}{\kappa_1}\int_\infty \sum_{\mathbf{s}_2}\frac{1}{2}\sum_{m_1,m_2}|M^{(C)}|^2 \times\delta(E_0+\kappa_1-E_p-\kappa_2)p^2\,dp\,d\Omega_p. \qquad (9)$$

III. EXTREME-RELATIVISTIC KINEMATICS

Our goal is to extract the dominant behavior, exact in Z, of the cross sections Eqs. (8) and (9), for $\kappa_1 \gg 1$ (mathematically $\kappa_1\to\infty$). To this end, it is useful to express the matrix elements $M^{(1)}$ and $M^{(2)}$ in terms of the momentum transferred to the nucleus

$$\boldsymbol{\Delta}\equiv\boldsymbol{\kappa}_1-\boldsymbol{\kappa}_2-\mathbf{p}. \qquad (10)$$

By rearranging the integrand of $M^{(1)}$, Eq. (5) may be written

$$M^{(1)}=\int\int[e^{-i\mathbf{p}\cdot\mathbf{r}_2}u^{(-)}_{\mathbf{p}m_2}(\mathbf{r}_2)]^\dagger e^{i\boldsymbol{\Delta}\cdot\mathbf{r}_2}(\boldsymbol{\alpha}\cdot\mathbf{s}_2)e^{-i\boldsymbol{\kappa}_1\cdot\mathbf{r}_2} \times G(\mathbf{r}_2,\mathbf{r}_1;\Omega_1)e^{i\boldsymbol{\kappa}_1\cdot\mathbf{r}_1}(\boldsymbol{\alpha}\cdot\mathbf{s}_1)u_{\mathbf{o}m_1}(\mathbf{r}_1)\,d\mathbf{r}_1\,d\mathbf{r}_2, \qquad (11)$$

and similarly for $M^{(2)}$.

In the limit $\kappa_1\to\infty$, $|\boldsymbol{\Delta}|$ may either tend to infinity (if the angles between the vectors involved are kept fixed), or may remain finite (if the angles are allowed to decrease conveniently in the process). However, the values of $M^{(1)}$ and $M^{(2)}$ at finite $|\boldsymbol{\Delta}|$ are dominant over those for $|\boldsymbol{\Delta}|\to\infty$. Indeed, in the latter case the rapid oscillations of the exponential $e^{i\boldsymbol{\Delta}\cdot\mathbf{r}_2}$ in Eq. (11) have an annihilating effect on the integral, as opposed to the former case. Since we are interested in a result to dominant order in $(1/\kappa_2)$, we shall consider the case

$$\kappa_1\to\infty, \quad \Delta=\text{finite}; \qquad (12)$$

this we shall designate as the *ER limit*.

The ER calculation of the matrix element and cross sections depends on the range of the scattered photon spectrum considered. One can distinguish three main ranges.

(i) The *soft-photon end*, defined by

$$\kappa_2<\epsilon, \qquad (13)$$

where $\epsilon>0$ and sufficiently small. In this range, the Compton effect and photoeffect, having the same initial conditions, are connected theoretically by the "soft-photon theorem." On the other hand, because any photon detector has necessarily an energy resolution threshold ε_d below which it cannot detect anything, for $\kappa_2<\varepsilon_d$, the Compton effect cannot be distinguished experimentally from the photoeffect (the quantities ϵ and ε_d are unrelated). This scattering regime will be discussed in Sec. VII.

From Eq. (2) it follows that in this case p takes the maximum possible value at given κ_1. In the ER limit, we have $p\cong\kappa_1\to\infty$. Moreover, by combining this with Eqs. (10) and (12), we find $\mathbf{p}\cdot\boldsymbol{\kappa}_1\cong p\kappa_1$, i.e., $\mathbf{p}$ is quasiparallel to $\boldsymbol{\kappa}_1$ in the angular range which gives the dominant contribution to the cross section.

(ii) The *range of the Compton line*, defined by $\eta\equiv(\kappa_2/\kappa_1)=\text{const}$, with η such that

$$\epsilon'<\eta<1-\varpi, \qquad (14)$$

where ϵ' and ϖ are positive, sufficiently small quantities. We shall show further that this spectral range covers, indeed, the profile of the Compton line.

Equation (14) implies that κ_2 is obliged to tend to infinity concomitantly with κ_1. From Eq. (2), we obtain in the ER limit

$$p\cong(1-\eta)\kappa_1\to\infty, \qquad (15)$$

$$\begin{aligned}\mathbf{p}\cdot\boldsymbol{\kappa}_1&\equiv\kappa_1^2-\boldsymbol{\kappa}_1\cdot\boldsymbol{\kappa}_2-\boldsymbol{\kappa}_1\cdot\boldsymbol{\Delta}\\&=\kappa_1^2(1-\eta\boldsymbol{\nu}_1\cdot\boldsymbol{\nu}_2)-\boldsymbol{\kappa}_1\cdot\boldsymbol{\Delta}\\&\cong\kappa_1^2(1-\eta)=p\kappa_1,\end{aligned} \qquad (16)$$

where we have used the notation Eq. (10), and

$$\boldsymbol{\nu}_i\equiv\boldsymbol{\kappa}_i/\kappa_i \quad (i=1,2). \qquad (17)$$

This shows that $\mathbf{p}$ and $\boldsymbol{\kappa}_1$ are again quasiparallel in the ER limit.

(iii) The *tip of the spectrum*, located in the vicinity of $\kappa_2^{\max}=E_0+\kappa_1-1$, hence having $p\cong 0$. In this vicinity, $\kappa_2\cong\kappa_1\to\infty$, but $\eta<1$ (strictly). This case will be discussed in Sec. VII.

We shall now derive some kinematic relations for the range of the Compton line. To this end, we shall consider $\boldsymbol{\kappa}_1$, $\boldsymbol{\kappa}_2$, and $\boldsymbol{\Delta}$, as the variables characterizing the scattering, instead of the original set $\boldsymbol{\kappa}_1$, $\boldsymbol{\kappa}_2$, and $\mathbf{p}$. Let us therefore change the integration variables accordingly in Eq. (9). The *energy conservation δ function* can be written as

$$\begin{aligned}&\delta\{E_0+\kappa_1-\kappa_2-[p^2+1]^{1/2}\}\\&\quad=2(E_0+\kappa_1-\kappa_2)\,\delta\{(p^2+1)-(E_0+\kappa_1-\kappa_2)^2\}.\end{aligned} \qquad (18)$$

By eliminating here p in favor of $\boldsymbol{\Delta}$, we have

$$\begin{aligned}&\delta\{(p^2+1)-(E_0+\kappa_1-\kappa_2)^2\}\\&\quad=\delta\{2\kappa_1\kappa_2(1-\boldsymbol{\nu}_1\cdot\boldsymbol{\nu}_2)-2E_0(\kappa_1-\kappa_2)\\&\qquad-2\boldsymbol{\Delta}\cdot(\boldsymbol{\kappa}_1-\boldsymbol{\kappa}_2)+(\Delta^2+a^2)\}.\end{aligned} \qquad (19)$$

Further, defining the unit vector $\mathbf{u}$, and the cosine w of its angle with $\boldsymbol{\Delta}$, by

$$\mathbf{u}\equiv(\boldsymbol{\nu}_1-\eta\boldsymbol{\nu}_2)/|\boldsymbol{\nu}_1-\eta\boldsymbol{\nu}_2|, \quad w\equiv\mathbf{u}\cdot(\boldsymbol{\Delta}/\Delta), \qquad (20)$$

the right-hand side of Eq. (19) can be transformed into

$$\delta\left\{2\kappa_1|\boldsymbol{\nu}_1-\eta\boldsymbol{\nu}_2|\Delta\left[w-\frac{1}{\Delta|\boldsymbol{\nu}_1-\eta\boldsymbol{\nu}_2|}\left(\kappa_2(1-\boldsymbol{\nu}_1\cdot\boldsymbol{\nu}_2)\right.\right.\right.$$
$$\left.\left.\left.-E_0(1-\eta)+\frac{(\Delta^2+a^2)}{2\kappa_1}\right)\right]\right\}$$
$$=\frac{1}{2\kappa_1|\boldsymbol{\nu}_1-\eta\boldsymbol{\nu}_2|\Delta}\,\delta\left\{w-\frac{1}{|\boldsymbol{\nu}_1-\eta\boldsymbol{\nu}_2|\Delta}\right.$$
$$\left.\times\left(\eta\xi-E_0(1-\eta)+\frac{(\Delta^2+a^2)}{2\kappa_1}\right)\right\}. \tag{21}$$

We have introduced here the notation

$$\xi\equiv\kappa_1(1-\boldsymbol{\nu}_1\cdot\boldsymbol{\nu}_2)=2\kappa_1\sin^2\frac{\theta}{2}, \tag{22}$$

where θ is the angle between the unit vectors $\boldsymbol{\nu}_1$ and $\boldsymbol{\nu}_2$. As we are operating under the condition Eq. (14), we have $|\boldsymbol{\nu}_1-\eta\boldsymbol{\nu}_2|\neq 0$. Note that we have made no approximations in handling the δ function, Eq. (18).

Returning to the cross section Eq. (8) and inserting Eqs. (18)–(21) in it, we find

$$d^4\tilde{\sigma}=\alpha^2\frac{\kappa_2}{\kappa_1}\sum_{\mathbf{s}_2}\frac{1}{2}\sum_{m_1,m_2}|M_{\rm ER}^{(C)}|^2\frac{(\gamma+\kappa_1-\kappa_2)}{\kappa_1|\boldsymbol{\nu}_1-\eta\boldsymbol{\nu}_2|\Delta}$$
$$\times\delta\left\{w-\frac{1}{|\boldsymbol{\nu}_1-\eta\boldsymbol{\nu}_2|\Delta}\left(\eta\xi-\gamma(1-\eta)\right.\right.$$
$$\left.\left.+\frac{(\Delta^2+a^2)}{2\kappa_1}\right)\right\}d\kappa_2\,d\Omega_2\;\Delta^2\,d\Delta\,d\Omega_\Delta, \tag{23}$$

containing the ER form of the matrix element. In Eq. (23), we have replaced E_0 by γ.

The δ function in Eq. (23) allows us to draw important kinematic conclusions. If the unit vector $\boldsymbol{\nu}_2$ is situated in an angular range such that $(1-\boldsymbol{\nu}_1\cdot\boldsymbol{\nu}_2)$ stays finite (finite angle scattering), we have $\xi\to\infty$ in the ER limit, and the value of w for which the δ function becomes singular is pushed to infinity, and hence lies outside its allowed interval of variation $(-1\leqslant w\leqslant+1)$. Therefore, the δ function will reduce the value of the cross section Eq. (23) to zero. However, if $\boldsymbol{\nu}_2$ varies in an angular range defined by

$$(1-\boldsymbol{\nu}_1\cdot\boldsymbol{\nu}_2)=O(1/\kappa_1), \tag{24}$$

ξ will be finite, and the singularity of the δ function can be made to lie within the interval $(-1\leqslant w\leqslant+1)$, so that the cross section Eq. (23) be nonvanishing. We conclude that, in the ER limit, the range of $\boldsymbol{\nu}_2$ that gives dominant contribution to the cross section is small-angle scattering: $\boldsymbol{\nu}_2\cong\boldsymbol{\nu}_1$. As θ is small, one gets from Eq. (22) the connection

$$\xi\simeq\kappa_1(\theta^2/2). \tag{25}$$

Thus, the δ function plays a double role in Eq. (23).

(a) It fixes the value of w in the matrix element $M_{\rm ER}^{(C)}$ at

$$\tilde{w}\equiv\frac{1}{|\boldsymbol{\nu}_1-\eta\boldsymbol{\nu}_2|\Delta}\left(\eta\xi-\gamma(1-\eta)+\frac{(\Delta^2+a^2)}{2\kappa_1}\right); \tag{26}$$

we shall denote the result of this replacement by $\tilde{M}_{\rm ER}^{(C)}$.

(b) It confines the integration over Δ, as $\tilde{w}$ needs to satisfy

$$-1\leqslant\tilde{w}\leqslant 1. \tag{27}$$

This leads to a limitation on Δ.

The exact form of the δ function in Eq. (23), and hence Eqs. (26) and (27), contains corrective terms $O(1/\kappa_1)$. Since we are interested in obtaining a consistent result only to dominant order in $1/\kappa_1$, it would appear that these terms should be discarded. However, as will become apparent in Sec. V, there is a peculiar increase of order of magnitude of the matrix element and cross sections when passing from $\xi\neq 0$ to $\xi=0$, and the corrective term in Eq. (26) is needed for a proper handling of this passage. We shall, therefore, keep it until it is safe to discard it.

When dealing solely with the case $\xi\neq 0$, we can use instead of $\tilde{w}$ of Eq. (26) the expression

$$\tilde{w}^0\equiv\frac{q}{\Delta},\quad q\equiv\frac{\eta}{(1-\eta)}\xi-\gamma. \tag{28}$$

[Recall that, according to condition Eq. (14), we have to lowest order in $1/\kappa_1$: $|\boldsymbol{\nu}_1-\eta\boldsymbol{\nu}_2|=(1-\eta)$.] In this approximation $\mathbf{u},\boldsymbol{\nu}_1,\boldsymbol{\nu}_2$ coincide, so that $\tilde{w}^0$ is the angle of $\boldsymbol{\Delta}$ with any one of them. From Eq. (27) we get

$$\Delta\geqslant|q|. \tag{29}$$

Note that when the cross section Eq. (8) is expressed in terms of the variables $\boldsymbol{\kappa}_1$, $\boldsymbol{\kappa}_2$, and $\mathbf{p}$, the energy conserving δ function places a constraint on p at given κ_1,κ_2. In the new variables $\boldsymbol{\kappa}_1$, $\boldsymbol{\kappa}_2$, and $\boldsymbol{\Delta}$, this is translated into a constraint on the direction of $\boldsymbol{\Delta}$, which should be at fixed angle with $\mathbf{u}$, given by Eq. (26). (Because of the quasiparallelism of $\boldsymbol{\nu}_1$ and $\boldsymbol{\nu}_2$, $\boldsymbol{\Delta}$ is approximately also at fixed angle with $\boldsymbol{\nu}_1$.) However, the magnitude of $\boldsymbol{\Delta}$ is required to be in excess of $|q|$, Eq. (28).

By integrating over w in Eq. (23), we get a new quadruply differential cross section

$$\frac{d^4\tilde{\sigma}_{ER}}{d\kappa_2\,d\Omega_2\;d\Delta\,d\Phi}=\alpha^2\,\eta\frac{(\gamma+\kappa_1-\kappa_2)}{\kappa_1|\boldsymbol{\nu}_1-\eta\boldsymbol{\nu}_2|}\Delta\sum_{\mathbf{s}_2}\frac{1}{2}\sum_{m_1,m_2}|\tilde{M}_{\rm ER}^{(C)}|^2. \tag{30}$$

We choose a reference frame that has the z axis along the vector $\mathbf{u}$, Eq. (20), and $\boldsymbol{\nu}_1$ and $\boldsymbol{\nu}_2$ in the Oxz plane; the polar angles of $\boldsymbol{\Delta}$ are $\Theta\equiv\arccos w$, and Φ. The doubly differential cross section Eq. (9) can then be written

$$\frac{d^2\sigma_{ER}}{d\kappa_2\, d\Omega_2}=\alpha^2\eta\int_{|q|}^{\infty}\Delta d\Delta\int_0^{2\pi}d\Phi\sum_{\mathbf{s}_2}\frac{1}{2}\sum_{m_1,m_2}|\tilde{M}_{\rm ER}^{(C)}|^2. \tag{31}$$

In passing from Eq. (30) to Eq. (31) we have used Eq. (29), and the fact that now $|\boldsymbol{\nu}_1-\eta\boldsymbol{\nu}_2|\simeq(1-\eta)$.

We note that already Heisenberg and Pauli, Sec. 1 of Ref. [10], had realized that Eqs. (12), (14), and (24), were the key conditions needed to define the ER limit of the Compton line for bound electrons, although no proof was given.

IV. MATRIX ELEMENT FOR THE RANGE OF THE COMPTON LINE

To derive the ER form of the matrix element for the *range of the Compton line*, case (ii), it is convenient to express the Green's function $G(\mathbf{r},\mathbf{r}';\Omega)$ and the continuum spinor $u_{\mathbf{p}m}^{(-)}(\mathbf{r})$, appearing in Eq. (11), in terms of the corresponding quantities $G^I(\mathbf{r},\mathbf{r}';\Omega)$ and $u_{\mathbf{p}m}^{I\,(-)}(\mathbf{r})$, for the iterated (second order) Dirac equation. For the Coulomb potential the (homogeneous/inhomogeneous) form of the iterated equation can be written as [e.g., see Ref. [6], Eq. (14.21), or Ref. [27(a)]], Eq. (3.6)]

$$[\Delta+(W+a/r)^2-I+ia\boldsymbol{\alpha}\cdot\mathbf{r}/r^3]\Xi^I=YI. \tag{32}$$

Per definition, $G^I(\mathbf{r},\mathbf{r}';\Omega)$ satisfies this equation with $\Xi^I\equiv G^I(\mathbf{r},\mathbf{r}';W)$, $W\equiv\Omega$, $Y\equiv\delta(\mathbf{r}-\mathbf{r}')\,I$, and $u_{\mathbf{p}m}^{I\,(-)}(\mathbf{r})$ with $\Xi^I\equiv u_{\mathbf{p}m}^{I\,(-)}(\mathbf{r})$, $W\equiv E_p=(p^2+1)^{1/2}$, $Y=0$. The connection between G^I and G is [28]

$$G=-(\boldsymbol{\alpha}\cdot\mathbf{P}+\beta+a/r_2+\Omega)\beta G^I\beta, \tag{33}$$

and that between $u_{\mathbf{p}m}^{I\,(-)}$ and $u_{\mathbf{p}m}^{(-)}$

$$u_{\mathbf{p}m}^{(-)}=-\frac{1}{2}(\boldsymbol{\alpha}\cdot\mathbf{P}+\beta+a/r+\Omega)\beta\, u_{\mathbf{p}m}^{I\,(-)}. \tag{34}$$

Thus, the matrix element Eq. (11) can be written as

$$\begin{aligned}M^{(1)}=\frac{1}{2}\int\int&[e^{-i\mathbf{p}\cdot\mathbf{r}_2}\{\boldsymbol{\alpha}\cdot\mathbf{P}_2+\beta+a/r_2+E_p\}\beta u_{I\mathbf{p}m_2}^{(-)}(\mathbf{r}_2)]^{\dagger}\\&\times e^{i\boldsymbol{\Delta}\cdot\mathbf{r}_2}(\boldsymbol{\alpha}\cdot\mathbf{s}_2)e^{-i\boldsymbol{\kappa}_1\cdot\mathbf{r}_2}\{\boldsymbol{\alpha}\cdot\mathbf{P}_2+\beta+a/r_2+\Omega_1\}\\&\times\beta G_I(\mathbf{r}_2,\mathbf{r}_1;\Omega_1)\beta e^{i\boldsymbol{\kappa}_1\cdot\mathbf{r}_1}(\boldsymbol{\alpha}\cdot\mathbf{s}_1)u_{om_1}(\mathbf{r}_1)d\mathbf{r}_1\,d\mathbf{r}_2,\end{aligned} \tag{35}$$

and similarly for $M^{(2)}$.

G^I and $u_{\mathbf{p}m}^{I\,(-)}$ satisfy an integral Lippmann-Schwinger type of equation following from Eq. (32), the usefulness of which will become apparent shortly. Defining

$$R(\mathbf{r})\equiv ia\boldsymbol{\alpha}\cdot\mathbf{r}/r^3+a^2/r^2, \tag{36}$$

the integral equation can be written in operator form as

$$\Xi^I=\Xi_0^I+G_0IR\Xi^I. \tag{37}$$

Here Ξ_0^I is a solution of the equation

$$\left[\Delta+\frac{2aW}{r}+(W^2-1)\right]\Xi_0^I=Y, \tag{38}$$

and G_0 is the Green's function associated with it. For the Green's function case $[Y=\delta(\mathbf{r}-\mathbf{r}')I]$ we need set $\Xi_0^I\equiv G_0(\mathbf{r}_2,\mathbf{r}_1;\Omega)I$, while for the the continuum spinor case $(Y=0)$ we need set $\Xi_0^I\equiv u_{\mathbf{p}}^{(-)}(\mathbf{r})\chi$. Here $G_0(\mathbf{r}_2,\mathbf{r}_1;\Omega)$ and $u_{\mathbf{p}}^{(-)}(\mathbf{r})$ are solutions of the ordinary (nonspinor) equation associated with Eq. (38), and χ is an arbitrary constant spinor. χ should be chosen such that the Dirac spinor $u_{\mathbf{p}m}^{(-)}$ in Eq. (34) reduces asymptotically to a normalized free particle spinor $\chi_{\mathbf{p}m}$ of the Dirac equation, Eq. (7), with momentum $\mathbf{p}$ and spin projection m on the z axis, as required by the matrix element Eq. (4). This can be achieved by choosing $\chi=\chi_{\mathbf{p}m}$, and thus $\Xi_0^I\equiv u_{\mathbf{p}}^{(-)}(\mathbf{r})\;\chi_{\mathbf{p}m}$ [see also the comments following Eq. (49) below]. From Eq. (38) it follows that $(-\Xi_0^I/2)$ satisfies the homogeneous/inhomogeneous Schrödinger equation for a Coulomb potential, in which the charge a and energy E have been modified according to

$$a\Rightarrow aW,\quad E\Rightarrow\tfrac{1}{2}(W^2-1). \tag{39}$$

We shall integrate in the following the matrix elements $M^{(1)},M^{(2)}$, in momentum space. By Fourier transforming we have

$$\begin{aligned}M^{(1)}=\frac{1}{2}\int\int&[\{\boldsymbol{\alpha}\cdot\mathbf{q}+\beta+V(\mathbf{q})+E_p\}\beta u_{\mathbf{p}m_2}^{I\,(-)}(\mathbf{q})]^{\dagger}(\boldsymbol{\alpha}\cdot\mathbf{s}_2)\\&\times\{\boldsymbol{\alpha}\cdot(\mathbf{p}_2+\boldsymbol{\kappa}_1)+\beta+V(\mathbf{p}_2+\boldsymbol{\kappa}_1)+\Omega_1\}\beta\\&\times G^I(\mathbf{p}_2+\boldsymbol{\kappa}_1,\mathbf{p}_1+\boldsymbol{\kappa}_1;\Omega_1)\\&\times\beta(\boldsymbol{\alpha}\cdot\mathbf{s}_1)u_{om_1}(\mathbf{p}_1)d\mathbf{p}_1\,d\mathbf{p}_2,\end{aligned} \tag{40}$$

$$\begin{aligned}M^{(2)}=\frac{1}{2}\int\int&[\{\boldsymbol{\alpha}\cdot\mathbf{q}+\beta+V(\mathbf{q})+E_p\}\beta u_{\mathbf{p}m_2}^{I\,(-)}(\mathbf{q})]^{\dagger}(\boldsymbol{\alpha}\cdot\mathbf{s}_1)\\&\times\{\boldsymbol{\alpha}\cdot(\mathbf{p}_2-\boldsymbol{\kappa}_2)+\beta+V(\mathbf{p}_2-\boldsymbol{\kappa}_2)+\Omega_2\}\beta\\&\times G^I(\mathbf{p}_2-\boldsymbol{\kappa}_2,\mathbf{p}_1-\boldsymbol{\kappa}_2;\Omega_2)\,\beta(\boldsymbol{\alpha}\cdot\mathbf{s}_2)u_{om_1}(\mathbf{p}_1)d\mathbf{p}_1\,d\mathbf{p}_2,\end{aligned} \tag{41}$$

with the notation $\mathbf{q}\equiv\mathbf{p}_2+\mathbf{p}+\boldsymbol{\Delta}$. $V(\mathbf{q})$ is the integral operator in momentum space corresponding to $V(r)\equiv-a/r$, see Ref. [9], Eq. (12). Equations (40) and (41) are still exact.

Let us now consider the ER limit of the matrix elements Eqs. (40) and (41). For the *Green's function* G^I we shall use the momentum-space form of Eq. (37). Its first term $\Xi_0^I\equiv G_0(\mathbf{p}_2,\mathbf{p}_1;\Omega)I$ contains the nonrelativistic momentum-space Coulomb Green's function with *modified parameters* as in Eq. (39), for which we can use the integral representation of Schwinger [29] and Hostler [27], see also Ref. [8(a)], Eqs. (18)–(20),

$$G_0(\mathbf{p}_2,\mathbf{p}_1;\Omega)\equiv -\frac{X^3}{4\pi^2}\int_0^1 \rho^{-\tau}\frac{d}{d\rho}\left(\frac{1-\rho^2}{\rho}\frac{1}{[X^2(\mathbf{p}_1-\mathbf{p}_2)^2+(\mathbf{p}_1^2+X^2)(\mathbf{p}_2^2+X^2)(1-\rho)^2/4\rho]^2}\right)d\rho, \tag{42}$$

where $\tau\equiv a/X$, $X^2\equiv -2\Omega$, with Re$X>0$. By modifying the parameters according to Eq. (39), we have

$$X^2=1-\Omega^2, \quad \tau=a\Omega/X, \quad \mathrm{Re}\,X>0. \tag{43}$$

In fact, in Eqs. (40) and (41) we need the ER limits of $G^I(\mathbf{p}_2+\boldsymbol{\kappa}_1,\mathbf{p}_1+\boldsymbol{\kappa}_1;E_o+\kappa_1+i\varepsilon)$, and $G^I(\mathbf{p}_2-\boldsymbol{\kappa}_2,\mathbf{p}_1-\boldsymbol{\kappa}_2;E_o-\kappa_2-i\varepsilon)$. It was shown in Ref. [9] that only the first term of the integral equation for G^I, Eq. (37), contributes to these limits

$$\lim_{\kappa_1\to\infty} G^I(\mathbf{p}_2+\boldsymbol{\kappa}_1,\mathbf{p}_1+\boldsymbol{\kappa}_1;E_o+\kappa_1+i\varepsilon) = \lim_{\kappa_1\to\infty} G_0(\mathbf{p}_2+\boldsymbol{\kappa}_1,\mathbf{p}_1+\boldsymbol{\kappa}_1;E_o+\kappa_1+i\varepsilon)I, \tag{44}$$

$$\lim_{\kappa_2\to\infty} G^I(\mathbf{p}_2-\boldsymbol{\kappa}_2,\mathbf{p}_1-\boldsymbol{\kappa}_2;E_o-\kappa_2-i\varepsilon) = \lim_{\kappa_2\to\infty} G_0(\mathbf{p}_2-\boldsymbol{\kappa}_2,\mathbf{p}_1-\boldsymbol{\kappa}_2;E_o-\kappa_2-i\varepsilon)I, \tag{45}$$

if $\mathbf{p}_1$ and $\mathbf{p}_2$ belong to a finite domain; moreover, the limits are proportional to $(1/\kappa_1)$ and $(1/\kappa_2)$, respectively [see Ref. [9], Eqs. (16)–(25)]. Since the integrals, Eqs. (40) and (41), are assumed to be convergent, $\mathbf{p}_1$ and $\mathbf{p}_2$ vary essentially in a finite volume, as required by Eqs. (44) and (45). Therefore, we are in a position to replace in our calculation the relativistic G^I with the nonrelativistic $G_0 I$ with modified parameters, which represents a great simplification [30]. Note that we can use, indeed, Eq. (45) for the calculation of the matrix element Eq. (41), because, at finite η [see Eq. (14)], we also have $\kappa_2\to\infty$.

Turning now to the *final state spinor* $u^{I(-)}_{\mathbf{p}m}(\mathbf{q})$, we recall that in the case (ii) we are studying, $p\to\infty$. We shall again use Eq. (37) in momentum space. Its first term contains the nonrelativistic continuum Coulomb wave function $u^{(-)}_{\mathbf{p}}(\mathbf{q})$, which is the Fourier transform of $u^{(-)}_{\mathbf{p}}(\mathbf{r})=N_c e^{i\mathbf{p}\cdot\mathbf{r}}\,{}_1F_1(n,1;-i(pr+\mathbf{p}\cdot\mathbf{r}))$, e.g., see Ref. [6], Eq. (29.38); n is defined nonrelativistically as $n\equiv(a/ip)$. For momentum-normalization, we shall take

$$N_c\equiv-(2\pi)^{-3/2}e^{(\pi/2)|n|}\,\Gamma(1+i|n|). \tag{46}$$

By using a closed-loop integral representation for the confluent hypergeometric function ${}_1F_1$ [31], and taking its Fourier transform, one obtains [see Ref. [8(a)], Eq. (17)]:

$$u^{(-)}_{\mathbf{p}}(\mathbf{q})\equiv\frac{4pN_c}{(2\pi)^{3/2}}\oint_{\varepsilon\to 0}\left(\frac{y-1}{y}\right)^n \times\frac{1}{\{(\mathbf{q}-\mathbf{p}y)^2+[\varepsilon+ip(1-y)]^2\}^2}dy. \tag{47}$$

The integration contour encircles in counterclockwise sense the critical points $y=0$ and $y=1$ of the integrand, but leaves outside its pole; the principal value of the imaginary power n in the integrand should be taken. However, Eq. (47) should be entered in Eq. (36) with the relativistically modified value of the parameter n; this is

$$n\equiv aE_p/ip. \tag{48}$$

When considering the limit $p\to\infty$ of $u^{(-)}_{\mathbf{p}}(\mathbf{q})$, Eq. (47), it can be shown (as for the Green's function) that only the first term of Eq. (37) contributes, and we have

$$\lim_{p\to\infty}u^{I(-)}_{\mathbf{p}m}(\mathbf{p}+\mathbf{a})=\lim_{p\to\infty}u^{(-)}_{\mathbf{p}}(\mathbf{p}+\mathbf{a})\chi_{\mathbf{p}m}, \tag{49}$$

where $\mathbf{a}$ may be any finite vector [32]. In our case, see Eq. (40), $\mathbf{a}\equiv\mathbf{p}_2+\boldsymbol{\Delta}$, both $\mathbf{p}_2$ and $\boldsymbol{\Delta}$ being essentially finite. We can, therefore, use instead of the relativistic $u^{I(-)}_{\mathbf{p}m}$, the nonrelativistic $u^{(-)}_{\mathbf{p}}I$, which is again a great simplification [30]. This possibility is a consequence of condition Eq. (15), which forces $p\to\infty$.

We need to consider also the limits of the two curly-bracket operators in the integrand of Eq. (40). The one acting upon βG^I becomes to leading order $\kappa_1(\boldsymbol{\alpha}\cdot\boldsymbol{\nu}_1+1)$. As to the one acting upon $\beta u^{I(-)}_{\mathbf{p}m_2}(\mathbf{q})$, it reduces to $(\boldsymbol{\alpha}\cdot\mathbf{p}+\beta+E_p)$ [33]. Thus, on account of Eq. (49), the square bracket in Eq. (40) contains $u^{(-)}_{\mathbf{p}}(\mathbf{p}_2+\mathbf{p}+\boldsymbol{\Delta})$ multiplied by the spinor $(\boldsymbol{\alpha}\cdot\mathbf{p}+\beta+E_p)\,\beta\,\chi_{\mathbf{p}m_2}=2\chi_{\mathbf{p}m_2}$. For $p\to\infty$, $\lim\chi_{\mathbf{p}m_2}=\chi_{\mathbf{n}m_2}$, where $\chi_{\mathbf{n}m_2}$ has components $2^{-1/2}\{\zeta_{m_2};(\mathbf{n}\cdot\sigma)\zeta_{m_2}\}$; we have denoted $\mathbf{n}\equiv(\mathbf{p}p)$, and by ζ_{m_2} either (1,0) or (0,1), depending on whether $m_2=+\frac{1}{2}$, or $m_2=-\frac{1}{2}$.

For the *initial state spinor* $u_{om_1}(\mathbf{p})$ we need to use an *exact expression* in order to obtain the exact Z dependence of the matrix element. We use the integral representation [9]

$$u_{om_1}(\mathbf{q})=\left[f(q)+\frac{1}{2}g(q)\boldsymbol{\alpha}\cdot\mathbf{q}\right]\chi_{om_1}, \tag{50}$$

$$f(q)\equiv\frac{N_0 a}{\Gamma(1-\gamma)}\int_0^\infty x^{-\gamma}\frac{(1+x)}{[q^2+a^2(1+x)^2]^2}dx, \tag{51}$$

$$g(q)\equiv\frac{2N_0 a}{\Gamma(1-\gamma)}\frac{1}{1+\gamma}\int_0^\infty x^{-\gamma}\frac{1}{[q^2+a^2(1+x)^2]^2}dx; \tag{52}$$

here χ_{om_1} is the constant spinor for a free particle at rest, of components $\{\zeta_{m_1};0\}$, and N_0 is the normalization constant

$$N_0\equiv\frac{2^{\gamma+1/2}a^{3/2}}{\pi}\left[\frac{1+\gamma}{\Gamma(2\gamma+1)}\right]^{1/2}. \tag{53}$$

Equations (50)–(53) are obtained by starting from the K-shell spinor in coordinate space [e.g., see Ref. [34], Eqs. (14.3), (14.4), (14.39), or Sec. 5 of Ref. [12], using an integral representation for the power $r^{\gamma-1}$ it contains [see Ref. [35], p. 1, Eq. (5)], and Fourier transforming the result. (We note that the integral representation for $r^{\gamma-1}$ has been first used in this context by Boyer [16].) By introducing the integral representations for $f(q)$ and $g(q)$, we have achieved that their q dependence is similar to that of the nonrelativistic $1s$ eigenfunction in momentum space, which can be easily handled.

Finally, we get

$$M_{\rm ER}^{(1)}=\kappa_1 \lim\int\int \chi^{\dagger}_{\mathbf{n}m_2} u_{\mathbf{p}}^{(-)*}(\mathbf{p}_2+\mathbf{p}+\mathbf{\Delta})(\boldsymbol{\alpha}\cdot\mathbf{s}_2)(\boldsymbol{\alpha}\cdot\boldsymbol{\nu}_1+1)\times(\boldsymbol{\alpha}\cdot\mathbf{s}_1)G_0(\mathbf{p}_2+\boldsymbol{\kappa}_1,\,\mathbf{p}_1+\boldsymbol{\kappa}_1;\Omega_1)\times\left[f(p_1)+\frac{1}{2}g(p_1)\boldsymbol{\alpha}\cdot\mathbf{p}_1\right]\chi_{om_1}\,d\mathbf{p}_1\,d\mathbf{p}_2. \quad (54)$$

Proceeding similarly for $M_{\rm ER}^{(2)}$,

$$M_{\rm ER}^{(2)}=-\kappa_2 \lim\int \chi^{\dagger}_{\mathbf{n}m_2} u_{\mathbf{p}}^{(-)*}(\mathbf{p}_2+\mathbf{p}+\mathbf{\Delta})(\boldsymbol{\alpha}\cdot\mathbf{s}_1)(\boldsymbol{\alpha}\cdot\boldsymbol{\nu}_2+1)\times(\boldsymbol{\alpha}\cdot\mathbf{s}_2)G_0(\mathbf{p}_2-\boldsymbol{\kappa}_2,\mathbf{p}_1-\boldsymbol{\kappa}_2;\Omega_2)\times\left[f(p_1)+\frac{1}{2}g(p_1)\boldsymbol{\alpha}\cdot\mathbf{p}_1\right]\chi_{om_1}\,d\mathbf{p}_1\,d\mathbf{p}_2. \quad (55)$$

The symbol "lim" has been introduced here to recall that the integrals should be evaluated in the ER limit, i.e., by extracting their dominant behavior for κ_1,κ_2,p tending to infinity in the manner discussed.

We have shown in this section that, as stated in the Introduction, the calculation of the Compton line matrix element can be carried out with nonrelativistic wave functions and Green's function, with relativistically modified parameters. We also note that the ER matrix elements Eqs. (54) and (55) can also be derived by using in Eqs. (4) and (5), the Sommerfeld-Maue approximations (see Chap. 5, Sec. 8 of Ref. [4] and Sec. 14.5 of Ref. [6]) for the final state Dirac spinor $u_{\mathbf{p}m_2}^{(-)\dagger}(\mathbf{r}_2)$, and Green's operator $G(\mathbf{r}_2,\mathbf{r}_1;\Omega)$.

V. REDUCTION OF THE MATRIX ELEMENT FOR THE RANGE OF THE COMPTON LINE TO SINGLE INTEGRALS

We shall now carry out the evaluation of the integrals in Eqs. (54) and (55). The four-component spinors χ_{om_1} and $\chi_{\mathbf{n}m_2}$ entering here can be expressed in terms of the two-component spinors ζ_m introduced in the preceding section. By expressing also the $\boldsymbol{\alpha}$ matrices in terms of 2×2 σ matrices, after some manipulation the matrix elements can be written as

$$M_{\rm ER}^{(1)}=\lim \zeta^{\dagger}_{m_2}[P+i\boldsymbol{\sigma}\cdot\boldsymbol{Q}]\zeta_{m_1}, \quad (56)$$

$$M_{\rm ER}^{(2)}=-\lim \zeta^{\dagger}_{m_2}[P'+i\boldsymbol{\sigma}\cdot\boldsymbol{Q}']\zeta_{m_1}, \quad (57)$$

where

$$P=\frac{1}{\sqrt{2}}\Big\{[(\mathbf{s}_1\cdot\mathbf{s}_2)(1-\boldsymbol{\nu}_1\cdot\mathbf{n})+(\mathbf{s}_1\cdot\mathbf{n})(\mathbf{s}_2\cdot\boldsymbol{\nu}_1)]A+\frac{1}{2}\{[\boldsymbol{B}\cdot(\mathbf{n}-\boldsymbol{\nu}_1)](\mathbf{s}_1\cdot\mathbf{s}_2)+(\mathbf{s}_1\cdot\boldsymbol{B})[\mathbf{s}_2\cdot(\mathbf{n}+\boldsymbol{\nu}_1)]-(\mathbf{s}_2\cdot\boldsymbol{B})(\mathbf{s}_1\cdot\mathbf{n})\}\Big\}, \quad (58)$$

$$\boldsymbol{Q}=\frac{1}{\sqrt{2}}\Big\{\{-(\mathbf{s}_1\times\mathbf{s}_2)+[\boldsymbol{\nu}_1\cdot(\mathbf{s}_1\times\mathbf{s}_2)]\mathbf{n}+(\mathbf{s}_2\cdot\boldsymbol{\nu}_1)(\mathbf{n}\times\mathbf{s}_1)-(\mathbf{s}_1\cdot\mathbf{s}_2)(\mathbf{n}\times\boldsymbol{\nu}_1)\}A+\frac{1}{2}\{[\boldsymbol{\nu}_1\cdot(\mathbf{s}_1\times\mathbf{s}_2)]\boldsymbol{B}-[(\mathbf{s}_1\times\mathbf{s}_2)\cdot\boldsymbol{B}]\mathbf{n}+(\mathbf{s}_1\cdot\boldsymbol{B})(\mathbf{n}\times\mathbf{s}_2)-(\mathbf{s}_2\cdot\boldsymbol{B})(\mathbf{n}\times\mathbf{s}_1)\}+\frac{1}{2}[(\mathbf{s}_1\cdot\mathbf{s}_2)(\mathbf{n}-\boldsymbol{\nu}_1)+(\mathbf{s}_2\cdot\boldsymbol{\nu}_1)\mathbf{s}_1]\times\boldsymbol{B}\Big\}. \quad (59)$$

We have introduced here the notation

$$A\equiv\kappa_1\int\int u_{\mathbf{p}}^{(-)*}(\mathbf{p}_2-\boldsymbol{\kappa}_2)G_0(\mathbf{p}_2,\mathbf{p}_1;\Omega_1)\times f(\mathbf{p}_1-\boldsymbol{\kappa}_1)d\mathbf{p}_1 d\mathbf{p}_2, \quad (60)$$

$$\boldsymbol{B}\equiv\kappa_1\int\int u_{\mathbf{p}}^{(-)*}(\mathbf{p}_2-\boldsymbol{\kappa}_2)G_0(\mathbf{p}_2,\mathbf{p}_1;\Omega_1)(\mathbf{p}_1-\boldsymbol{\kappa}_1)\times g(\mathbf{p}_1-\boldsymbol{\kappa}_1)d\mathbf{p}_1 d\mathbf{p}_2. \quad (61)$$

P' and $\boldsymbol{Q}'$ are obtained from P and $\boldsymbol{Q}$ by changing $\boldsymbol{\nu}_1$ into $\boldsymbol{\nu}_2$, interchanging $\mathbf{s}_1$ and $\mathbf{s}_2$, and replacing the integrals A, $\boldsymbol{B}$, by $A',\boldsymbol{B}'$; the latter are obtained from A,$\boldsymbol{B}$,by changing $\boldsymbol{\kappa}_2$ into $-\boldsymbol{\kappa}_1$, $\boldsymbol{\kappa}_1$ into $-\boldsymbol{\kappa}_2$ (hence κ_1 into κ_2), and Ω_1 into Ω_2. No approximations were done in passing from Eqs. (54) and (55) to Eqs. (56) and (57).

Integral $\boldsymbol{B}$ can be expressed as a linear combination of the vectors $\boldsymbol{\kappa}_1$, $\boldsymbol{\kappa}_2$, and $\mathbf{p}$, it contains. For consistency, we shall introduce instead $\boldsymbol{\kappa}_1$, $\boldsymbol{\kappa}_2$, and $\mathbf{\Delta}$, or rather their unit vectors $\boldsymbol{\nu}_1$, $\boldsymbol{\nu}_2$, and $\boldsymbol{\delta}\equiv\mathbf{\Delta}/\Delta$. Thus

$$\boldsymbol{B}\equiv d_1\boldsymbol{\nu}_1+d_2\boldsymbol{\nu}_2+d_3\boldsymbol{\delta}. \quad (62)$$

Insertion of this into Eqs. (58) and (59), will give the complete dependence of P and $\boldsymbol{Q}$ on the unit vectors of the problem, $\mathbf{s}_1,\mathbf{s}_2,\boldsymbol{\nu}_1,\boldsymbol{\nu}_2,\boldsymbol{\delta}$. Note that $\mathbf{n}$ can be expressed in terms of the latter by using Eq. (10):

$$\mathbf{n}\equiv\frac{\mathbf{p}}{p}=\frac{\kappa_1}{p}\boldsymbol{\nu}_1-\frac{\kappa_2}{p}\boldsymbol{\nu}_2-\frac{\Delta}{p}\boldsymbol{\delta}. \quad (63)$$

In view of Eq. (15), the first two terms here are $O(1)$, while the last one is $O(1/\kappa_1)$.

We proceed to derive the ER limits of $P, \boldsymbol{Q}, P', \boldsymbol{Q}'$. In these expressions, we need to consider, on the one hand, the integrals $A,\boldsymbol{B}$, and on the other, the factors containing products of unit vectors multiplying the integrals (we shall call these "unit-vector factors"). In the process we shall take into account the limitations imposed by the energy-conserving δ function of Eq. (23), as discussed in Sec. III.

We start by deriving the *ER dominant behavior of the unit-vector factors*. Scalar products like $(\mathbf{s}_1\cdot\boldsymbol{\nu}_2),(\mathbf{s}_2\cdot\boldsymbol{\nu}_1)$, are exactly 0 for $\xi=0$. At $\xi\neq 0$, they can be evaluated by introducing a reference frame consisting of $\boldsymbol{\nu}_1$, and two orthogonal polarization vectors $\mathbf{s}_1', \mathbf{s}_1''$, chosen such that $\boldsymbol{\nu}_2$ be in the plane of $\boldsymbol{\nu}_1$ and $\mathbf{s}_1'$. Under these circumstances $\boldsymbol{\nu}_2^2=(\boldsymbol{\nu}_2\cdot\boldsymbol{\nu}_1)^2+(\boldsymbol{\nu}_2\cdot\mathbf{s}_1')^2$, and hence, with Eq. (26), we have $(\boldsymbol{\nu}_2\cdot\mathbf{s}_1')=O(1/\sqrt{\kappa_1})$. Since an arbitrary polarization vector $\mathbf{s}_1$ is a linear combination of $\mathbf{s}_1'$ and $\mathbf{s}_1''$, also $(\boldsymbol{\nu}_2\cdot\mathbf{s}_1)=O(1/\sqrt{\kappa_1})$. In the case of $(\boldsymbol{\nu}_1\times\boldsymbol{\nu}_2)$, one can use $(\boldsymbol{\nu}_1\times\boldsymbol{\nu}_2)^2=1-(\boldsymbol{\nu}_1\cdot\boldsymbol{\nu}_2)^2=(\xi/\kappa_1)(1+\boldsymbol{\nu}_1\cdot\boldsymbol{\nu}_2)$ to show it to be $O(1/\sqrt{\kappa_1})$. Similarly, we find that products like $(\mathbf{s}_1\cdot\mathbf{n})$, $(\mathbf{s}_2\cdot\mathbf{n}),(\mathbf{n}\times\boldsymbol{\nu}_1),(\mathbf{n}\times\boldsymbol{\nu}_2)$, are of order $O(1/\sqrt{\kappa_1})$, and so is the magnitude of the vectors $(\boldsymbol{\nu}_1-\boldsymbol{\nu}_2),(\mathbf{n}-\boldsymbol{\nu}_1),(\mathbf{n}-\boldsymbol{\nu}_2)$. On the other hand, products like $(\mathbf{s}_1\cdot\mathbf{s}_2),(\boldsymbol{\nu}_1\times\mathbf{s}_1),(\mathbf{n}\times\mathbf{s}_1)$, $(\mathbf{s}_1\cdot\boldsymbol{\delta}),(\boldsymbol{\delta}\cdot\boldsymbol{\nu}_1)$, etc., are $O(1)$, irrespective of ξ. We need to deal also with combinations like $(1-\boldsymbol{\nu}_1\cdot\mathbf{n})$ and $(1-\boldsymbol{\nu}_2\cdot\mathbf{n})$. With Eqs. (63) and (15), we find at $\xi\neq 0$ that they are $O(1/\kappa_1)$. A careful analysis shows that at $\xi=0$, $(1-\boldsymbol{\nu}_1\cdot\mathbf{n})=(1-\boldsymbol{\nu}_2\cdot\mathbf{n})=O(1/\kappa_1^2)$.

Proceeding along these lines, and keeping only the dominant unit-vector factors, we find in the ER limit

$$P_{\rm ER}\equiv\lim P=\lim\frac{1}{2\sqrt{2}}\frac{d_3}{1-\eta}\{\eta(\mathbf{s}_1\cdot\mathbf{s}_2)[\boldsymbol{\delta}\cdot(\boldsymbol{\nu}_1-\boldsymbol{\nu}_2)]+(2-\eta)(\mathbf{s}_1\cdot\boldsymbol{\delta})(\mathbf{s}_2\cdot\boldsymbol{\nu}_1)+\eta(\mathbf{s}_2\cdot\boldsymbol{\delta})(\mathbf{s}_1\cdot\boldsymbol{\nu}_2)\},\tag{64}$$

$$\boldsymbol{Q}_{\rm ER}\equiv\lim\boldsymbol{Q}=\lim\frac{1}{\sqrt{2}}[K_1\boldsymbol{\nu}_1+K_2\mathbf{s}_1+K_3(\boldsymbol{\nu}_1\times\mathbf{s}_1)],\tag{65}$$

where

$$K_1=-\frac{1}{2}d_3\Big\{2[\mathbf{s}_1\cdot(\boldsymbol{\nu}_1\times\boldsymbol{\delta})](\mathbf{s}_2\cdot\boldsymbol{\nu}_1)+\frac{\eta}{1-\eta}(\mathbf{s}_1\cdot\mathbf{s}_2)[\boldsymbol{\delta}\cdot(\boldsymbol{\nu}_1\times\boldsymbol{\nu}_2)]+\frac{\eta}{1-\eta}[(\mathbf{s}_1\times\mathbf{s}_2)\cdot\langle\boldsymbol{\nu}_1(\boldsymbol{\delta}\cdot\boldsymbol{\nu}_2)-\boldsymbol{\nu}_2(\boldsymbol{\delta}\cdot\boldsymbol{\nu}_1)\rangle]\Big\},\tag{66}$$

$$K_2=\frac{\eta}{2(1-\eta)}\{-[2A-(d_1+d_2)][\mathbf{s}_2\cdot(\boldsymbol{\nu}_1\times\boldsymbol{\nu}_2)]\}+\frac{\eta}{2(1-\eta)}d_3\{[(\mathbf{s}_1\times\mathbf{s}_2)\cdot\boldsymbol{\delta}](\mathbf{s}_1\cdot\boldsymbol{\nu}_2)+(\mathbf{s}_1\cdot\mathbf{s}_2)\langle\mathbf{s}_1\cdot[(\boldsymbol{\nu}_1-\boldsymbol{\nu}_2)\times\boldsymbol{\delta}]\rangle\},\tag{67}$$

$$K_3=\frac{2-\eta}{2(1-\eta)}[2A-(d_1+d_2)-d_3(\boldsymbol{\delta}\cdot\boldsymbol{\nu}_1)](\mathbf{s}_2\cdot\boldsymbol{\nu}_1).\tag{68}$$

Similarly, we obtain

$$P'_{\rm ER}\equiv\lim P'=\lim\frac{1}{2\sqrt{2}}\frac{d_3'}{1-\eta}[(\mathbf{s}_1\cdot\mathbf{s}_2)\langle\boldsymbol{\delta}\cdot(\boldsymbol{\nu}_1-\boldsymbol{\nu}_2)\rangle+(1-2\eta)(\mathbf{s}_1\cdot\boldsymbol{\nu}_2)(\mathbf{s}_2\cdot\boldsymbol{\delta})-(\mathbf{s}_1\cdot\boldsymbol{\delta})(\mathbf{s}_2\cdot\boldsymbol{\nu}_1)],\tag{69}$$

where d_1', d_2', d_3' are the components of $\boldsymbol{B}'$ in a decomposition as in Eq. (62). Using further a decomposition for $\boldsymbol{Q}'_{\rm ER}\equiv\lim\boldsymbol{Q}'$ with respect to the same unit vectors as in Eq. (65), we find at $\xi\neq 0$:

$$K_1'=\frac{1}{2}d_3'\Big\{[\mathbf{s}_1\cdot(\boldsymbol{\nu}_1\times\boldsymbol{\delta})](\mathbf{s}_2\cdot\boldsymbol{\nu}_1)-[\mathbf{s}_2\cdot(\boldsymbol{\nu}_1\times\boldsymbol{\delta})](\mathbf{s}_1\cdot\boldsymbol{\nu}_2)-\frac{1}{1-\eta}(\mathbf{s}_1\cdot\mathbf{s}_2)[\boldsymbol{\delta}\cdot(\boldsymbol{\nu}_1\times\boldsymbol{\nu}_2)]+\frac{\eta}{1-\eta}(\mathbf{s}_1\times\mathbf{s}_2)\cdot\langle\boldsymbol{\nu}_1(\boldsymbol{\delta}\cdot\boldsymbol{\nu}_2)-\boldsymbol{\nu}_2(\boldsymbol{\delta}\cdot\boldsymbol{\nu}_1)\rangle\Big\},\tag{70}$$

$$K_2'=\frac{1}{2(1-\eta)}[2A'-(d_1'+d_2')]\{2\eta\boldsymbol{\nu}_1\cdot(\mathbf{s}_1\times\mathbf{s}_2)(\mathbf{s}_1\cdot\boldsymbol{\nu}_2)-[\mathbf{s}_2\cdot(\boldsymbol{\nu}_1\times\boldsymbol{\nu}_2)]\}+\frac{1}{2(1-\eta)}d_3'\{(2\eta-1)[(\mathbf{s}_1\times\mathbf{s}_2)\cdot\boldsymbol{\delta}]\times(\mathbf{s}_1\cdot\boldsymbol{\nu}_2)+(\mathbf{s}_1\cdot\mathbf{s}_2)\langle\mathbf{s}_1\cdot[(\boldsymbol{\nu}_1-\boldsymbol{\nu}_2)\times\boldsymbol{\delta}]\rangle\},\tag{71}$$

$$K_3'=-\frac{1}{2(1-\eta)}[2A'-(d_1'+d_2')-d_3'(\boldsymbol{\delta}\cdot\boldsymbol{\nu}_1)]\times[2\eta(\mathbf{s}_1\cdot\mathbf{s}_2)(\mathbf{s}_1\cdot\boldsymbol{\nu}_2)+(\mathbf{s}_2\cdot\boldsymbol{\nu}_1)].\tag{72}$$

As easily seen, the unit-vector factors retained in Eqs. (64)–(72) are all of order $O(1/\sqrt{\kappa_1})$ at $\xi\neq 0$. However, they *all vanish at* $\xi=0$, to $O(1/\sqrt{\kappa_1})$. By considering the corrections to the unit-vector factors, it is not difficult to see that their true order of magnitude at $\xi=0$ is $O(1/\kappa_1)$.

We now turn to the evaluation of the *ER dominant behavior of the integrals* $A, \boldsymbol{B}, A', \boldsymbol{B}'$. We shall illustrate on the case of A how these sixfold integrals can be reduced analytically to single integrals. For similar procedures see Ref. [8], Sec. III, and Ref. [9], Sec. IV. By inserting the integral representations Eqs. (42), (47), and (50), (51), into Eq. (60), and inverting the order of integrations, we find

$$A=\mathcal{N}\int_0^\infty dx\,x^{-\gamma}\Lambda\int_0^1 d\rho\,\rho^{-\tau_1}\oint_{\varepsilon\to 0}dy\left(\frac{y-1}{y}\right)^{-n}\times\frac{1}{4\mu\Lambda}\frac{\partial^2}{\partial\Lambda\,\partial\mu}\frac{d}{d\rho}\left(\frac{1-\rho^2}{\rho}J(X^2,\Lambda,\mu)\right),\tag{73}$$

where

$$J(X^2,\Lambda,\mu)\equiv\int\int\frac{d\mathbf{p}_1\,d\mathbf{p}_2}{[(\mathbf{p}_2-\overline{\boldsymbol{\kappa}_2})^2+\mu^2][X_1^2(\mathbf{p}_1-\mathbf{p}_2)^2+\alpha(\mathbf{p}_1^2+X_1^2)(\mathbf{p}_2^2+X_1^2)]^2[(\mathbf{p}_2-\boldsymbol{\kappa}_1)^2+\Lambda^2]},\tag{74}$$

and

$$\mathcal{N}=-\frac{1}{\pi^2(2\pi)^{3/2}\Gamma(1-\gamma)}p\kappa_1X_1^3N_0N_c^*.\tag{75}$$

We have also denoted $\overline{\boldsymbol{\kappa}_2}\equiv\boldsymbol{\kappa}_2+\mathbf{p}y$, $\mu\equiv\varepsilon-ip(1-y)$, $\alpha\equiv(1-\rho)^2/4\rho$, $\Lambda\equiv a(1+x)$. In the ER limit, the parameters entering here are [see Eqs. (43) and (48)] $n=-ia$, $X_1=-i\kappa_1$, $\tau_1=ia$, for integral A, and $n=-ia$, $X_2=-i\kappa_2$, $\tau_2=-ia$, for integral A'. It is understood that the limit $\varepsilon\to0$ in Eq. (73) should be taken after performing the derivatives with respect to ρ,μ,Λ.

The momentum integral Eq. (74) was encountered and calculated elsewhere [36]. Using Eq. (23) given there [see also Ref. [8], Eqs. (33) and (34)], we have for our J in Eq. (74), see Ref. [37],

$$\frac{d}{d\rho}\left(\frac{1-\rho^2}{\rho}J(X^2,\Lambda,\mu)\right)=\frac{16\pi^4}{X^2}\frac{1}{c},$$

$$c\equiv[(X+\Lambda)^2+\kappa_1^2][(X+\mu)^2+\overline{\kappa_2^2}]-2\rho[4(\boldsymbol{\kappa}_1\cdot\overline{\boldsymbol{\kappa}_2})X^2+(\Lambda^2+\kappa_1^2-X^2)(\mu^2+\overline{\kappa_2^2}-X^2)]+\rho^2[(X-\Lambda)^2+\kappa_1^2][(X-\mu)^2+\overline{\kappa_2^2}].\tag{76}$$

This gives further

$$A=\mathcal{N}\int_0^\infty dx\,x^{-\gamma}\int_0^1 d\rho\,\rho^{-\tau_1}\oint_{\varepsilon\to0}dy\left(\frac{y-1}{y}\right)^{-n}\frac{1}{y-1}\times\left\{\frac{u_0+u_1y+u_2y^2}{c^3}-\frac{v_0+v_1y}{c^2}\right\},\tag{77}$$

where u_i,v_i, are polynomials in x and ρ of at most second degree, which do not depend on y.

The contour integration over the variable y in Eq. (77) can be performed analytically, by applying the residue theorem. Since c has the form $c\equiv c_0(y-y_0)$, the integrand is analytic with respect to y outside the integration contour throughout the whole complex y plane, with the exception of the pole at y_0, and vanishes as $1/y^2$ at infinity. The residue theorem can be applied by closing the contour at infinity; the calculation is quite tedious.

As a result, in the ER limit, the integrand of the integral over ρ in Eq. (77) has the form $[R(\rho)]^{ia}Q(\rho)$, where $R(\rho)$ and $Q(\rho)$ are complicated rational functions. Surprisingly enough, we could find a function $U(\rho)$ such that $dU(\rho)/d\rho=\{[R(\rho)]^{ia}Q(\rho)\}_{\rm ER}$, which makes the integration trivial. One is thus left in the expression of $A_{\rm ER}=\lim A$ with a single integral.

The final expressions of $A_{\rm ER}$ and $A'_{\rm ER}$ are

$$A_{\rm ER}=\frac{N}{\eta\mathcal{Z}}A^0_{\rm ER},\quad A'_{ER}=-\frac{\eta N}{\mathcal{Z}'}A^0_{\rm ER},\tag{78}$$

where

$$A^0_{\rm ER}=\int_0^\infty x^{-\gamma}\left[\frac{\Delta^2+\Lambda^2}{\boldsymbol{\Delta}\cdot\boldsymbol{\nu}_1-i\Lambda}\right]^{ia}\times\left[\frac{2(1-ia)\Lambda}{(\Delta^2+\Lambda^2)^2}+\frac{a}{(\boldsymbol{\Delta}\cdot\boldsymbol{\nu}_1-i\Lambda)(\Delta^2+\Lambda^2)}\right]dx\tag{79}$$

and

$$N=\frac{\pi^{3/2}N_0N_c^*}{\sqrt{2}[2\kappa_1(1-\eta)]^{ia}\Gamma(1-\gamma)},\tag{80}$$

$$\mathcal{Z}=\gamma+\boldsymbol{\Delta}\cdot\boldsymbol{\nu}_2+\xi,\quad\mathcal{Z}'=\gamma+\boldsymbol{\Delta}\cdot\boldsymbol{\nu}_1-\eta\xi.\tag{81}$$

A similar procedure can be followed in the calculation of $\boldsymbol{B}$. We find

$$\boldsymbol{B}_{\rm ER}=\frac{N}{\eta\mathcal{Z}}\boldsymbol{B}^0_{\rm ER},\quad\boldsymbol{B}'_{\rm ER}=-\frac{\eta N}{\mathcal{Z}'}\boldsymbol{B}^0_{\rm ER}.\tag{82}$$

We give the components of $\boldsymbol{B}^0_{ER}$, in a decomposition similar to Eq. (62). In fact, only d_1+d_2 and d_3 are needed in Eqs. (66)–(68), Ref. [38], given by

$$d_1^0+d_2^0=-\frac{2ia^2}{1+\gamma}\int_0^\infty x^{-\gamma}\left[\frac{\Delta^2+\Lambda^2}{\boldsymbol{\Delta}\cdot\boldsymbol{\nu}_1-i\Lambda}\right]^{ia}\times\frac{1}{(\Delta^2+\Lambda^2)(\boldsymbol{\Delta}\cdot\boldsymbol{\nu}_1-i\Lambda)}dx,\tag{83}$$

$$d_3^0=-\frac{4a(1-ia)\Delta}{1+\gamma}\int_0^\infty x^{-\gamma}\left[\frac{\Delta^2+\Lambda^2}{\boldsymbol{\Delta}\cdot\boldsymbol{\nu}_1-i\Lambda}\right]^{ia}\frac{1}{(\Delta^2+\Lambda^2)^2}dx.\tag{84}$$

Equations (78) and (82) represent the dominant behavior in $1/\kappa_1$ of the integrals $A_{\rm ER},A'_{\rm ER},\boldsymbol{B}_{\rm ER},\boldsymbol{B}'_{\rm ER}$. They undergo a peculiar change of order of magnitude in their ξ dependence at $\xi=0$. By taking into account the constraint imposed by the δ function Eq. (23), the integrals $A^0_{\rm ER},A'^0_{\rm ER},\boldsymbol{B}^0_{\rm ER},\boldsymbol{B}'^0_{\rm ER}$ are $O(1)$, irrespective of the value of ξ. This means that we can replace the $\boldsymbol{\Delta}\cdot\boldsymbol{\nu}_1$ they contain by $\boldsymbol{\Delta}\cdot\mathbf{u}$, and use the approximate form $\tilde{w}^0$ of Eq. (28), yielding $\boldsymbol{\Delta}\cdot\boldsymbol{\nu}_1\cong\mathbf{q}$. The denominators $\mathcal{Z},\mathcal{Z}'$, Eq. (81), give rise to problems, however. We first calculate *exactly* the quantities $\boldsymbol{\Delta}\cdot\boldsymbol{\nu}_1,\boldsymbol{\Delta}\cdot\boldsymbol{\nu}_2$ they contain, using the exact expression of $\boldsymbol{\Delta}\cdot\mathbf{u}\equiv\tilde{w}$ in Eq. (26). This gives

$$\mathcal{Z}=\xi\frac{1}{1-\eta}+\frac{1}{\kappa_1}\frac{\Delta^2+a^2}{2(1-\eta)}+O_h, \tag{85}$$

$$\mathcal{Z}'=\xi\frac{\eta^2}{1-\eta}+\frac{1}{\kappa_1}\frac{\Delta^2+a^2}{2(1-\eta)}+O_h', \tag{86}$$

where O_h and O_h' contain terms of higher order in ξ, and $1/\kappa_1$. Evidently, at $\xi\neq 0$, $\mathcal{Z}$ and $\mathcal{Z}'$ are $O(1)$ with respect to $1/\kappa_1$. However, these $O(1)$ terms vanish at $\xi=0$, which means a change of order of magnitude for the integrals $A_{\rm ER}$, $A'_{\rm ER}, \boldsymbol{B}_{\rm ER}, \boldsymbol{B}'_{\rm ER}$. Thus, the correct order of magnitude of the integrals is $O(1)$ at $\xi\neq 0$, and $O(\kappa_1)$ at $\xi=0$.

We now combine these findings for the integrals with the behavior, discussed earlier, of the unit-vector factors. At $\xi\neq 0$ we conclude that the order of magnitude of the matrix elements $M_{\rm ER}^{(1)}, M_{\rm ER}^{(2)}$ is $O(1/\sqrt{\kappa_1})$. On the other hand, we have found that at $\xi=0$ the unit-vector factors change of order of magnitude, becoming $O(1/\kappa_1)$ (we have not calculated them in this case, however). Taking into account also the change of order of magnitude of the integrals, we find that the order of magnitude of the matrix elements $M_{\rm ER}^{(1)}$, $M_{\rm ER}^{(2)}$ at $\xi=0$ *increases* to $O(1)$. Correspondingly, the differential cross section Eq. (31) will rise from $O(1/\kappa_1)$ at $\xi\neq 0$, to $O(1)$ at $\xi=0$.

Unfortunately, we are not in a position to handle the case of $\xi=0$ with our approximate formulas. This would require to include consistently all corrective terms of $O(1/\kappa_1)$ to the unit-vector factors calculated. To this end one would need to start from Eqs. (40) and (41), with the corrected expressions Eq. (37) for G^I and $u_{\mathbf{p}m}^{I(-)}$, rather than from Eqs. (54) and (55), as we have done. Therefore, we shall restrict ourselves in the following to $\xi\neq 0$. In this case, Eqs. (85) and (86) become, to dominant order,

$$\mathcal{Z}=\xi\frac{1}{1-\eta},\quad \mathcal{Z}'=\xi\frac{\eta^2}{1-\eta}. \tag{87}$$

Note that these expressions can be obtained directly from Eq. (81) by taking into account that at $\xi\neq 0$ we can approximate $\boldsymbol{\Delta}\cdot\boldsymbol{\nu}_1\cong\boldsymbol{\Delta}\cdot\boldsymbol{\nu}_2\cong\boldsymbol{\Delta}\cdot\mathbf{u}\cong q$, and then use Eq. (28).

VI. DOUBLY DIFFERENTIAL CROSS SECTION FOR THE RANGE OF THE COMPTON LINE

Having obtained the ER expression of the matrix element, we are now in a position to derive the cross sections, Eqs. (30) and (31), at $\xi\neq 0$. The first step is the summation over the electron polarizations. In view of Eqs. (56) and (57), and by using well-known summation formulas, we have

$$\frac{1}{2}\sum_{m_1,m_2}|\tilde{M}_{\rm ER}^{(1)}+\tilde{M}_{\rm ER}^{(2)}|^2=|P_{\rm ER}-P'_{\rm ER}|^2+|\boldsymbol{Q}_{\rm ER}-\boldsymbol{Q}'_{\rm ER}|^2. \tag{88}$$

Note that, since at this stage we have taken into account the restrictions imposed by the δ function of Eq. (23), we are entitled to place a tilde over $M_{ER}^{(1)}, M_{ER}^{(2)}$. The next step is the summation over $\mathbf{s}_2$, which is a straightforward, albeit very tedious calculation. The result is rather compact

$$\sum_{\mathbf{s}_2}\frac{1}{2}\sum_{m_1,m_2}|\tilde{M}_{\rm ER}^{(1)}+\tilde{M}_{\rm ER}^{(2)}|^2\cong\frac{(1+\eta^2)}{\kappa_1\eta^2\xi}T, \tag{89}$$

where

$$T=|N|^2\left\{|2A_{\rm ER}^0-[(d_1^0+d_2^0)+d_3^0\tilde{w}^0]|^2+\left(1-\frac{q^2}{\Delta^2}\right)|d_3^0|^2\right\}, \tag{90}$$

with q and $\tilde{w}^0$ defined by Eq. (28).

The quadruply differential cross section Eq. (30) can thus be written ($\xi\neq 0$)

$$\frac{d^4\tilde{\sigma}_{\rm ER}}{d\kappa_2\,d\Omega_2\,d\Delta\,d\Phi}=\alpha^2\frac{1}{\kappa_1}\frac{(1+\eta^2)}{\eta\,\xi}T\Delta. \tag{91}$$

To pass to Eq. (31), we have to carry out the integrals over Φ and Δ. That over Φ is trivial, as there is no Φ dependence left in our approximation. The final expression for the *ER doubly differential cross section* Eq. (31) at $\xi\neq 0$ reads

$$\frac{d^2\sigma_{\rm ER}}{d\kappa_2\,d\Omega_2}=2\pi\alpha^2\frac{1}{\kappa_1}\frac{(1+\eta^2)}{\eta\,\xi}\int_{|q|}^{\infty}T\Delta\,d\Delta. \tag{92}$$

The quantities entering Eq. (92) are defined by Eqs. (90), (79), (83), (84), (87), and (28). Note that there is no $\mathbf{s}_1$ dependence left in the expression of the cross section Eq. (92). As a consequence, the expression will also give the cross section averaged over the initial polarization $\mathbf{s}_1$.

We shall now show that the quantities h and d_3^0, entering the expression of T, can be expressed in terms of known transcendentals. This will allow the transformation of these expressions in view of a simpler computation. Let us consider, for example, d_3^0 of Eq. (84). By changing the integration variable, the integral can easily be recognized to be that of a generalized hypergeometric function of several variables $x_1,\ldots,x_n$, of the Lauricella type F_D, e.g., see Ref. [39], Chap. VII, Eq. (8),

$$F_D(a;b_1,\ldots,b_n;c;x_1,\ldots,x_n)=[\Gamma(c)/\Gamma(b)\Gamma(c-a)]\int_0^1\rho^{a-1}(1-\rho)^{c-a-1}\times(1-x_1\rho)^{-b_1}\cdots(1-x_n\rho)^{-b_n}\,d\rho. \tag{93}$$

We find, specifically,

$$d_3^0=-\frac{4a(1-ia)\Delta}{1+\gamma}\frac{(\Delta^2+a^2)^{ia-2}}{(q-ia)^{+ia}}\frac{\Gamma(1-\gamma)\Gamma(\gamma+3-ia)}{\Gamma(4-ia)}\times F_D(1-\gamma;2-ia,2-ia,ia;4-ia;x_1,x_2,x_3), \tag{94}$$

where

$$x_1 = \frac{\Delta}{\Delta + ia}, \quad x_2 = \frac{\Delta}{\Delta - ia}, \quad x_3 = \frac{q}{q - ia}. \tag{95}$$

However, because $c = b_1 + b_2 + b_3$, the F_D function of *three* variables in Eq. (94) reduces to a F_D function of *two* variables (also called Appell function F_1). Indeed [see Ref. [39], Chap. VII, Eq. (10_3)],

$$F_D(a;b_1,b_2,b_3;b_1+b_2+b_3;x_1,x_2,x_3) = (1-x_3)^{-a} F_1\left(a;b_1,b_2;b_1+b_2+b_3;\frac{x_1-x_3}{1-x_3},\frac{x_2-x_3}{1-x_3}\right). \tag{96}$$

Proceeding similarly in all cases, we get

$$T = |K|^2 \left\{ 4|L_1+L_2|^2 + \left(1 - \frac{q^2}{\Delta^2}\right)|L_3|^2 \right\}, \tag{97}$$

where

$$L_1 = \frac{2}{(\Delta^2+a^2)^2} \frac{1-ia}{3-ia} [(1+\gamma+q)(2+\gamma-ia)F^{(2)} + ia(q-ia)\, F^{(3)}], \tag{98}$$

$$L_2 = \frac{(1+\gamma+ia)}{(\Delta^2+a^2)(q-ia)} F^{(1)}, \tag{99}$$

$$L_3 = -\frac{4\Delta}{(\Delta^2+a^2)^2} \frac{1-ia}{3-ia} (2+\gamma-ia) F^{(2)}, \tag{100}$$

$$|K|^2 = \frac{a^5}{16\pi^2} \frac{2^{2\gamma}}{(1+\gamma)\Gamma(1+2\gamma)} \left(\frac{2\pi a}{1-e^{-2\pi a}} \right) \times \left| \frac{\Gamma(2+\gamma-ia)}{\Gamma(3-ia)} \right|^2 \left(\frac{a^2}{q^2+a^2} \right)^{\gamma-1} e^{2a\psi}. \tag{101}$$

We have denoted here

$$F^{(1)} \equiv F_1(1-\gamma;1-ia,1-ia;3-ia;z_+,z_-), \tag{102}$$

$$F^{(2)} \equiv F_1(1-\gamma;2-ia,2-ia;4-ia;z_+,z_-), \tag{103}$$

$$F^{(3)} \equiv F_1(2-\gamma;2-ia,2-ia;4-ia;z_+,z_-), \tag{104}$$

with

$$z_+ \equiv \frac{\Delta+q}{\Delta+ia}, \quad z_- \equiv \frac{\Delta-q}{\Delta-ia}, \tag{105}$$

and

$$\tan\psi = -(a/q), \quad -\pi \leqslant \psi \leqslant 0. \tag{106}$$

The final form of the cross section Eq. (92) has thus been expressed in terms of the quantities in Eqs. (97)–(105). Note that the integral over Δ in Eq. (92) is a function of a and q, and that ξ and η are contained only in q of Eq. (28). The evaluation of the Appell functions involved, as well as the integration over Δ, has to be carried out numerically. Our results will be presented in Sec. VIII.

We have stated that the spectral region *case* (ii), characterized by Eq. (14), contains the Compton line. This will be illustrated in Sec. VIII by the numerical results. Here, we shall check this in the *case of small a*. Using simple properties of the Appell functions F_1, it is easy to see that the dominant behavior of Eqs. (98)–(100) is

$$L_1 \simeq \frac{2(2+q)}{(\Delta^2+a^2)^2}, \quad L_2 \simeq \frac{2}{(q-ia)(\Delta^2+a^2)},$$

$$L_3 \simeq -\frac{4\Delta}{(\Delta^2+a^2)^2}. \tag{107}$$

Terms of order a have been neglected in the numerators. On the other hand, because of the resonant nature of the denominators, we shall use the exact form of q, see Eq. (28). We write $|K|^2$, Eq. (101), as

$$|K|^2 \equiv \frac{a^5}{16\pi^2} S(a) e^{2a\psi}. \tag{108}$$

$Q(a)$, as defined by the equation, tends to 1 for $a \to 0$. We leave its expression open, depending on the accuracy desired. We note, however, that Eq. (108) contains the exponentials $e^{2a\psi}$ and $e^{-2\pi a}$ whose exponents are quite large even for relatively small Z, so that it would be impractical to approximate them by 1.

Inserting Eq. (107) into the expression of T, Eq. (97), and performing the simple integration over Δ in Eq. (92), yields the small a cross section

$$\frac{d^2\sigma_{\rm ER}}{d\kappa_2\, d\Omega_2} = \frac{\alpha^2}{6\pi} a^5 S(a) e^{2a\psi} \frac{1}{\kappa_1} \frac{1+\eta^2}{(1-\eta)(q+1)} \times \frac{8+20q+15q^2}{(q^2+a^2)^3}. \tag{109}$$

Let us now go to the *free electron limit*, $a \to 0$. Equation (109) contains the functional representation of the $\delta(x)$ function

$$\delta(x) = \frac{8}{3\pi} \lim_{a\to 0} \frac{a^5}{(x^2+a^2)^3}. \tag{110}$$

Using well-known properties, we obtain

$$\lim_{a\to 0} \frac{d^2\sigma_{\rm ER}}{d\kappa_2\, d\Omega_2} = \frac{d\sigma_{ER}^{KN}}{d\Omega_2} \delta\left(\kappa_2 - \frac{\kappa_1}{1+\xi} \right), \tag{111}$$

$$\frac{d\sigma_{\rm ER}^{KN}}{d\Omega_2} \equiv \frac{1}{2}\alpha^2 \frac{1+(1+\xi)^2}{(1+\xi)^3}. \tag{112}$$

We recall that $\kappa_2=\kappa_1(1+\xi)^{-1}$ is the ER form of the Compton formula for the scattered photon frequency, and that $d\sigma_{\rm ER}^{KN}/d\Omega_2$ is the ER limit of the Klein-Nishina cross section (e.g., see Sec. 28.5 of Ref. [6]). Equation (111) then shows that, indeed, our cross section Eq. (92) covers the spectral region of the Compton line.

VII. LOW- AND HIGH-FREQUENCY ENDS OF THE SCATTERED PHOTON SPECTRUM

We now turn to the discussion of the limiting cases (i) and (iii) of Sec. III. *Case* (i) will be mentioned here only for the sake of completeness, as it has been treated elsewhere [19]. In principle, it requires a different calculation than we have done for the Compton line, as the condition $\eta>\epsilon'$ [i.e., $\kappa_2\to\infty$] of Eq. (14) assumed in the former is incompatible with $\kappa_2<\epsilon$ we now need. Neverthless, a closer look at the former calculation shows that the assumption $\kappa_2\to\infty$ was made only for $M^{(2)}$, see Eq. (45), and not for $M^{(1)}$. On the other hand, it is known that, of the two matrix elements $M^{(1)}$ and $M^{(2)}$, only $M^{(1)}$ (for "photon absorption first") contributes dominantly to the soft-photon limit, see Refs. [8(a)], [13(a)], [15]. Then, the cross section we need is given, to dominant order in $(1/\kappa_2)$, by Eq. (31) with $M^{(2)}$ neglected.

By leaving out the contribution of $M^{(2)}$ from our calculation, we find that the cross sections can be expressed as ($\xi\neq 0$)

$$\frac{d^4\sigma_{\rm ER}^{(C,\,IR)}}{d\kappa_2\,d\Omega_2\,d\Delta\,d\Phi}\cong\frac{\alpha}{2\pi^2}\frac{1}{\kappa_1\kappa_2}\frac{\Delta}{\xi}\frac{d\sigma_{\rm ER}^{(Ph)}}{d\Omega_{\mathbf{p}}},\qquad(113)$$

$$\frac{d^3\sigma_{\rm ER}^{(C,IR)}}{d\kappa_2\,d\Omega_2}\cong\frac{\alpha}{2\pi^2}\frac{\kappa_1}{\kappa_2}\frac{1}{\xi}\sigma_{\rm ER}^{(Ph)},\qquad(114)$$

where

$$\frac{d\sigma_{\rm ER}^{(Ph)}}{d\Omega_{\mathbf{p}}}\equiv(2\pi)^2\alpha\kappa_1 T^{(0)},\qquad(115)$$

$$\sigma_{\rm ER}^{(Ph)}\equiv\frac{(2\pi)^3\alpha}{\kappa_1}\int_\gamma^\infty T^{(0)}\Delta\,d\Delta.\qquad(116)$$

$T^{(0)}$ is the expression of T, Eqs. (97)–(105), taken at $\kappa_2=0$. Note that κ_2 is contained only in q of Eq. (28) which appears in the variables z_+,z_-, Eq. (105). Replacing in these quantities q by $-\gamma$ (its value at $\kappa_2=0$), they become

$$z_+^{(0)}=\frac{\Delta-\gamma}{\Delta+ia},\quad z_-^{(0)}=\frac{\Delta+\gamma}{\Delta-ia}.\qquad(117)$$

Thus, $T^{(0)}$ and the integral in Eq. (116) reduce to functions of a only.

The cross sections Eqs. (113) and (114) diverge as $(1/\kappa_2)$ in the soft photon limit; this is the "infrared divergence." Moreover, by comparing with results by Nagel [17] and Boyer [16], we have shown in Ref. [19] that the quantities $(d\sigma_{\rm ER}^{(Ph)}/d\Omega_{\mathbf{n}})$ and $\sigma_{\rm ER}^{(Ph)}$ represent, indeed, the ER limits of the differential and total photoeffect cross sections. We have shown there that Eqs. (113) and (114) are expressions of the "soft-photon theorem" in the ER domain.

We now turn to case (iii). We shall merely outline the calculation, for the sake of obtaining the order of magnitude of the result with respect to $(1/\kappa_1)$. Note that we cannot use our results for case (i) or (ii), since in these instances we have assumed $p\to\infty$. In the following $\mathbf{p}$ is considered to be a fixed, small vector.

Starting from Eqs. (4) and (5), we can again make appear in the integrals the momentum transfer Eq. (10). We again express the Dirac Green's function G in terms of that for the iterated equation G^I, Eq. (33), but we shall maintain the usual Dirac expression for the final state $u_{\mathbf{p}m_2}^{(-)}$. As $\kappa_2\cong\kappa_1\to\infty$, we can again apply Eqs. (44) and (45), to get the momentum space integral

$$M_{\rm ER}^{(1)}=\kappa_1\lim\int\int u_{\mathbf{p}m_2}^{(-)\dagger}(\mathbf{p}_2+\mathbf{p}+\mathbf{\Delta})(\boldsymbol{\alpha}\cdot\mathbf{s}_2)(\boldsymbol{\alpha}\cdot\boldsymbol{\nu}_1+1)\times(\boldsymbol{\alpha}\cdot\mathbf{s}_1)G_0(\mathbf{p}_2+\boldsymbol{\kappa}_1,\mathbf{p}_1+\boldsymbol{\kappa}_1;\Omega_1)\,u_{om_1}(\mathbf{p}_1)d\mathbf{p}_1\,d\mathbf{p}_2,\qquad(118)$$

and a similar expression for $M_{\rm ER}^{(2)}$. These are akin to the ones we used in the high-energy Rayleigh scattering calculation, see, Eqs. (27), (28), and (31) of Ref. [9] except that here the final state is different from the initial one and lies in the continuum. We can proceed by using the integral representations, Eqs. (42) and (50), for G_0 and u_{om_1}, of the present paper. This would allow an analytic handling of the matrix elements up to a certain point, beyond which a numerical evaluation will be needed.

The order of magnitude of matrix element Eq. (118) is different from that of the Compton line, because now the direction $\mathbf{n}$ is no longer quasiparallel to $\boldsymbol{\nu}_1$, but can be arbitrary. The unit-vector factors appearing in Eq. (118) are $O(1)$, and, as also the integrals they are multiplying are $O(1)$ [see Ref. [9], Sec. III], the whole matrix element Eq. (118) is now $O(1)$.

Thus, at the tip of the spectrum we find that the doubly differential cross section Eq. (9) is $O(1)$, irrespective of ξ, whereas for the contiguous spectral region of the Compton line, it was $O(1/\kappa_1)$ or $O(1)$, depending on whether $\xi\neq 0$ or $\xi=0$. This means that, for $\xi\neq 0$, there is an increase of order of magnitude of the cross section at the tip of the spectrum (similar to that occurring in the angular distribution at $\xi=0$). Note that this behavior will not show up in our numerical computations for the Compton line, as this effect is not contained in the formulas we shall be using.

VIII. RESULTS AND DISCUSSION

We now present the results of the numerical computation of the cross section Eq. (92). The Appell functions F_1 it contains were evaluated using their integral representation Eq. (93), combined with very accurate numerical integration routines.

For convenience of the graphical representation, we shall be considering the relative cross section

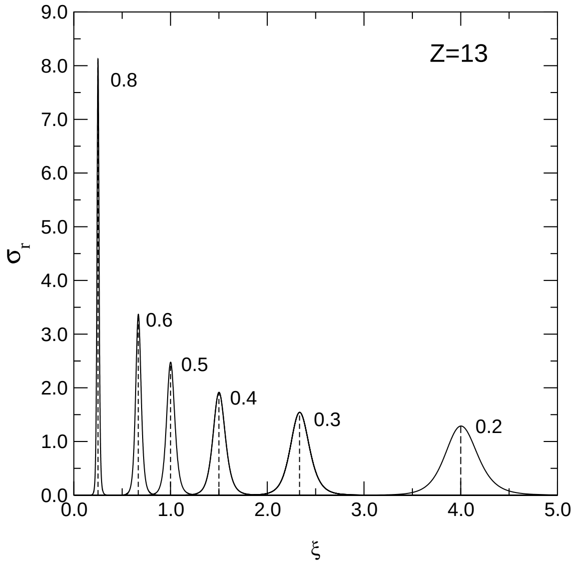

FIG. 1. Extreme-relativistic doubly differential Compton cross section σ_r, Eq. (119), for $Z=13$, at fixed values of $\eta=\kappa_2/\kappa_1$, indicated next to the Compton profiles, and variable ξ, Eq. (22). The dotted lines mark the locations of the corresponding free-electron Compton lines.

$$\sigma_r = \frac{d^2\sigma_{\mathrm{ER}}}{d\kappa_2\, d\Omega_2} \bigg/ \frac{4\,\alpha^2}{3\pi a \kappa_1}. \tag{119}$$

At given κ_1 and Z, σ_r is a function of the two independent variables ξ and η. Physically interesting are the sections through the surface $\sigma_r(\xi,\eta)$, at $\eta=$const (angular distributions), and $\xi=$const (spectral distributions). We have calculated σ_r for three typical values of $Z=13$ (Al), 50 (Sn), and 82 (Pb). We have cut off the infrared divergent behavior, which is anyway not covered correctly by the present computation (see Sec. VII); the cut off is noticeable only at high Z.

Figures 1–3 contain the *angular distributions*, at indicated η. The location of the free Compton line is shown by a dotted line. It is apparent that the height of the peak increases with increasing η, while its location ξ_{C} shifts towards smaller ξ, at all Z. In fact, ξ_{C} lies always very close to ξ_0, the location of the free electron line, $\xi_0=(1-\eta)/\eta$. The full width at half maximum (FWHM) of the line, $(\Delta\xi)_{\mathrm{C}}$, decreases as η increases.

Figures 4–6 give the *spectral distributions*, at indicated ξ. The location of the free Compton line is again marked by a dotted line. For all Z, the height of the peak decreases with increasing ξ, while its location η_{C} shifts towards larger η and then smaller η. Again, the location of η_C is very close to the location of the free electron line, $\eta_0=(1+\xi)^{-1}$. For all Z, the FWHM of the line $(\Delta\eta)_{\mathrm{C}}$ first increases with η, and then decreases.

The fact that the location of the Compton peak is unexpectedly so close to that of the free electron, for both distributions and at all Z, as well as the peculiar behavior of the widths $(\Delta\xi)_{\mathrm{C}}$ and $(\Delta\eta)_{\mathrm{C}}$ require attention. For a quantitative discussion, we list the pertinent quantities in Tables I and II.

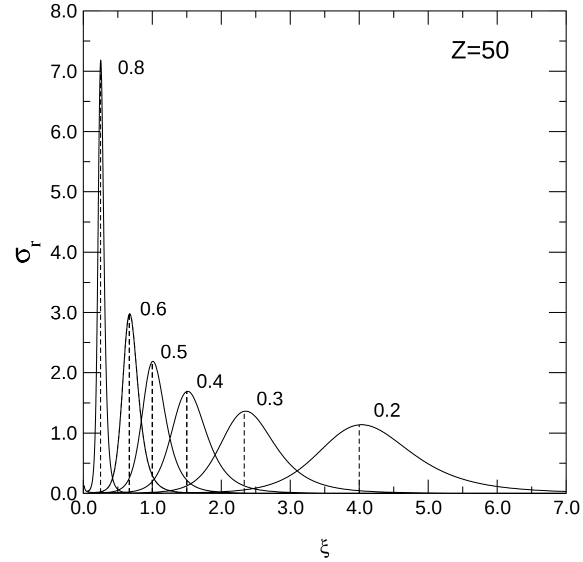

FIG. 2. The same as for Fig. 1, except that $Z=50$.

Let us start with the *Compton defect*, the shift of the Compton peak from the location of the free line, defined as $(\delta\xi)_{\mathrm{C}}\equiv\xi_C-\xi_0$ and $(\delta\eta)_{\mathrm{C}}\equiv\eta_C-\eta_0$. The Compton defect has attracted considerable interest at low photon energies (e.g., see Ref. [40] and references therein), theoretical and experimental. At low κ_1, the nonrelativistic defect for the unscreened Coulomb K shell is negative, and sizable. In the ER case, from Tables I and II, the Compton defect is positive and surprisingly small, as $(\delta\xi)_{\mathrm{C}}/\xi_0$ is less than 1%, and $(\delta\eta)_{\mathrm{C}}/\eta_0$ is less than 3%, for all Z. One may well wonder if this is not the reflection of some underlying physical argument requiring that, in the ER limit, the peak should occur at the location for the free particle (recall the question raised by Pauli and Heisenberg [10], mentioned in the Introduction). This, however, is not the case. On the one hand, the errors of our computation are considerably smaller than the values of

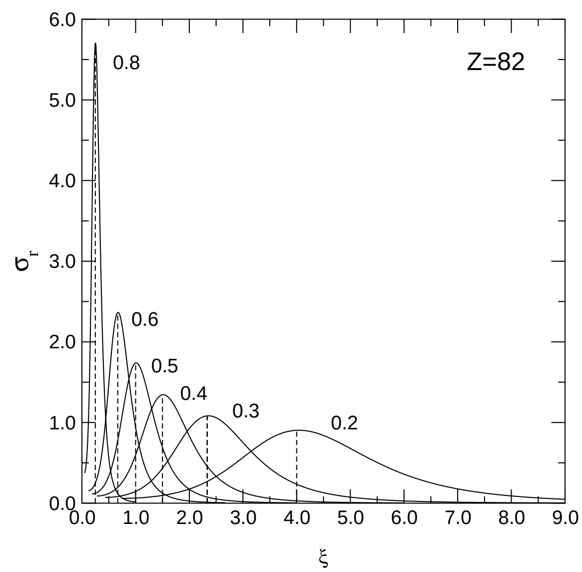

FIG. 3. The same as for Fig. 1, except that $Z=82$.

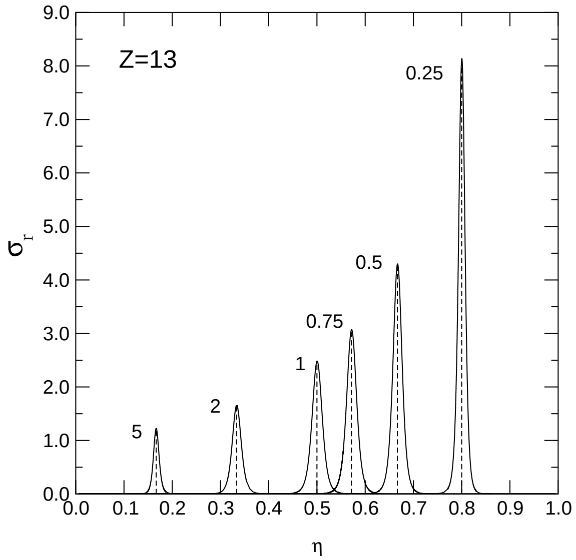

FIG. 4. Extreme-relativistic doubly differential Compton cross section σ_r, Eq. (119), for $Z=13$, at fixed values of ξ, Eq. (22), indicated next to the Compton profiles, and variable $\eta=\kappa_2/\kappa_1$. The dotted lines mark the locations of the corresponding free-electron Compton lines.

$(\delta\xi)_{\mathrm{C}}$ and $(\delta\eta)_{\mathrm{C}}$, so that these have to be considered truly nonzero. On the other hand, had this been the case, an analytic evaluation of the defect should give zero to all orders in a. We shall prove that this is not so, by obtaining analytic expressions for $(\delta\xi)_{\mathrm{C}}$ and $(\delta\eta)_{\mathrm{C}}$ to the lowest two nonvanishing orders in a.

The analytic evaluation of $(\delta\xi)_{\mathrm{C}}$ amd $(\delta\eta)_{\mathrm{C}}$ requires some care. In order that the result be consistent to a given order in a, one needs to start from an adequate approximation of the cross section. For example, Eq. (109) is a valid starting point for a calculation to $O(a^2)$. Indeed, let us first consider only the denominator of Eq. (109). This would indicate that the Compton peak would occur at $q=0$. The conclusion is illegitimate, however, because the terms linear in q in the numerator shift the maximum to a $q=O(a^2)$. Note that q dependence is contained also in the prefactor $(1+\eta^2)/(1-\eta)(q+1)$, as well as in $e^{2a\psi}$. Moreover, it turns out that it is sufficient to know the coefficients of the powers of q only to zeroth order in a. Equation (109) satisfies these requirements, and is thus capable of rendering correctly $(\delta\xi)_{\mathrm{C}}$ and $(\delta\eta)_{\mathrm{C}}$, to $O(a^2)$. If, on the other hand, one desires formulas valid to $O(a^4)$, one needs to proceed from the exact Eq. (92). A tedious calculation leads to

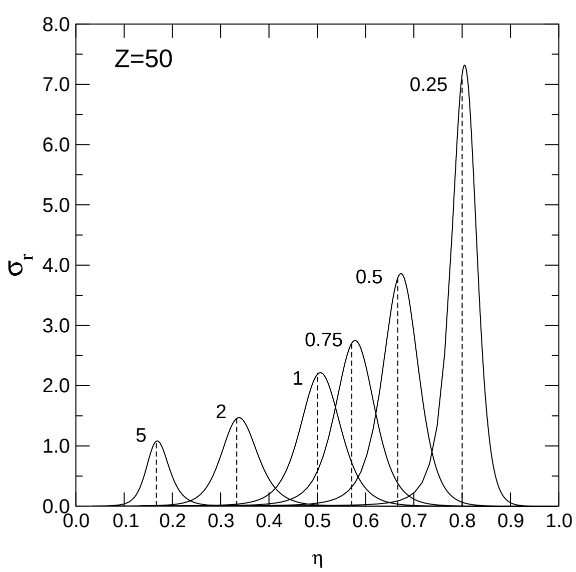

FIG. 5. The same as for Fig. 4, except that $Z=50$.

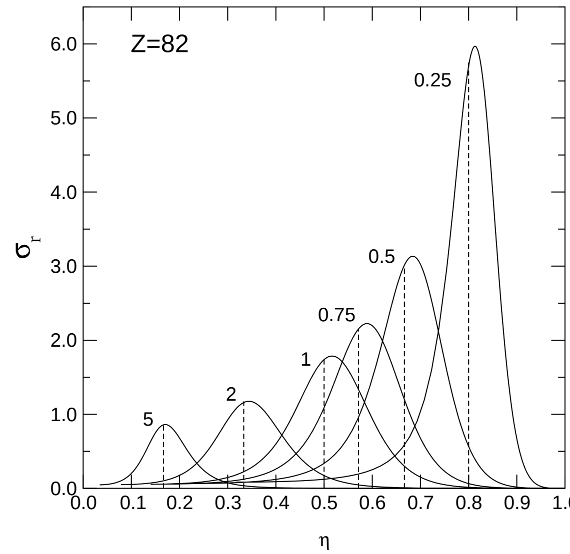

FIG. 6. The same as for Fig. 4, except that $Z=82$.

$$(\delta\xi)_{\mathrm{C}}^{\mathrm{an}}/\xi_0 \simeq \tfrac{1}{12}a^2-\tfrac{1}{8}a^4. \tag{120}$$

On the other hand, $(\delta\eta)_{\mathrm{C}}^{\mathrm{an}}/\eta_0$ is ξ dependent. We find

TABLE I. Characteristics of the *angular distribution* for the Compton line, at given Z and η. ξ_0 represents the location of the free-electron line; $(\delta\xi)_{\mathrm{C}}$ and $(\delta\xi)_{\mathrm{C}}^{\mathrm{an}}$ are Compton defects, from the computation, and according to Eq. (120); $(\Delta\xi)_{\mathrm{C}}$ and $(\Delta\xi)_{\mathrm{C}}^{\mathrm{an}}$ are FWHM, from the computation, and according to Eq. (123).

	η	ξ_0	$(\delta\xi)_{\mathrm{C}}$	$(\delta\xi)_{\mathrm{C}}^{\mathrm{an}}$	$(\Delta\xi)_{\mathrm{C}}$	$(\Delta\xi)_{\mathrm{C}}^{\mathrm{an}}$
$Z=13$						
	0.20	4	0.0030	0.0030	0.39	0.39
	0.50	1	0.0074	0.00074	0.095	0.097
	0.80	0.25	0.00018	0.00018	0.024	0.024
$Z=50$						
	0.20	4	0.035	0.035	1.58	1.49
	0.50	1	0.0087	0.0089	0.39	0.37
	0.80	0.25	0.0022	0.0022	0.099	0.093
$Z=82$						
	0.20	4	0.040	0.055	2.89	2.44
	0.50	1	0.011	0.014	0.72	0.61
	0.80	0.25	0.0025	0.0035	0.18	0.15

TABLE II. Characteristics of the *spectral distribution* for the Compton line, at given Z and ξ. η_0 represents the location of the free-electron line; $(\delta\eta)_C$ and $(\delta\eta)_C^{an}$ are Compton defects, from the computation, and according to Eq. (121), with the $O(a^4)$ term included; $(\Delta\eta)_C$ and $(\Delta\eta)_C^{an}$ are FWHM from the computation, and according to Eq. (123).

	ξ	η_0	$(\delta\eta)_C$	$(\delta\eta)_C^{an}$	$(\Delta\eta)_C$	$(\Delta\eta)_C^{an}$
$Z=13$						
	0.25	0.80	0.00035	0.00035	0.016	0.016
	1	0.50	0.00045	0.00045	0.024	0.024
	5	1.66	0.00015	0.00015	0.013	0.013
$Z=50$						
	0.25	0.80	0.0050	0.0049	0.061	0.060
	1	0.50	0.0064	0.0064	0.098	0.093
	5	1.66	0.0019	0.0020	0.055	0.052
$Z=82$						
	0.25	0.80	0.013	0.012	0.107	0.098
	1	0.50	0.016	0.016	0.17	0.15
	5	1.66	0.0039	0.042	0.101	0.085

$$(\delta\eta)_C^{an}/\eta_0 \simeq \frac{\xi(6+12\xi+5\xi^2+\xi^3)}{12(1+\xi)^2(2+2\xi+\xi^2)}a^2 + C(\xi)\,a^4; \tag{121}$$

the coefficient $C(\xi)$ has not been reproduced here because it is too complicated (it is the ratio of two ninth degree polynomials in ξ).

Thus, the Compton defects do not vanish to $O(a^4)$, as stated. The values yielded by the $O(a^4)$ formulas agree quite well with the computed ones even at large Z, as can be seen in Tables I and II. The tables emphasize the small numerical value of the defects $(\delta\xi)_C$ and $(\delta\eta)_C$. The reason for this is now apparent: on the one hand, the coefficients entering the analytic expansions in a^2 are small, and on the other hand, the terms tend to cancel each other.

The heights of the Compton peaks for the angular and spectral distributions of σ_r, denoted $\mathcal{H}_C$ and H_C, respectively, are according to Eqs. (109) and (119),

$$\mathcal{H}_C^{an} = S(a)e^{2a\psi}\frac{1+\eta^2}{1-\eta}, \quad H_C^{an} = S(a)e^{2a\psi}\frac{1+(1+\xi)^2}{\xi(1+\xi)}. \tag{122}$$

Their values are in good agreement with the numerical $\mathcal{H}_C$ and H_C.

We finally turn to the *FWHM of the Compton* line $(\Delta\xi)_C$ and $(\Delta\eta)_C$. From Eq. (109) we find to lowest order in a,

$$(\Delta\xi)_C^{an} \simeq 1.02\frac{1-\eta}{\eta}a, \quad (\Delta\eta)_C^{an} \simeq 1.02\frac{\xi}{(1+\xi)^2}a. \tag{123}$$

Tables I and II show that $(\Delta\xi)_C^{an}$ and $(\Delta\eta)_C^{an}$ agree very well at small a $(Z=13)$, with the exact widths, but that the agreement deteriorates at higher Z [with differences of order $O(a^2)$, as expected]. Equation (123) reveals the characteristics of the exact $(\Delta\xi)_C$, namely, its monotonic decrease with η, and the qualitative dependence of $(\Delta\eta)_C$ on ξ (e.g., its maximum at $\xi\simeq 1$).

We have thus shown that the elementary formulas Eqs. (109), (120)–(123), provide a good qualitative understanding of the characteristics of the ER Compton line. In fact, they even represent fairly adequate approximations.

ACKNOWLEDGMENTS

The authors are grateful to Richard H. Pratt for a collaboration extending over decades. They would also like to thank Alex Dalgarno for his hospitality at ITAMP. This work was partially supported by the National Science Foundation through a grant for ITAMP.

[1] B. Williams, *Compton Scattering* (McGraw-Hill, New York, 1977).
[2] M.J. Cooper, Rep. Prog. Phys. **48**, 415 (1984).
[3] P.M. Bergstrom and R.H. Pratt, in *Inelastic Scattering of X-rays and γ-rays*, special issue of Radiat. Phys. Chem. **50**, 3 (1997).
[4] A rather complete compilation of references was made by J.H. Hubbell, Radiat. Phys. Chem. **50**, 113 (1997). Early developments were recorded by A. Sommerfeld, *Atombau und Spektrallinien* (Vieweg, Braunschweig, 1939), Vol. II, Chap. VIII.
[5] (a) R. Ribberfors, Phys. Rev. A **12**, 2067 (1975); (b) **12**, 3136 (1975).
[6] A.I. Akhieser and V.B. Berestetskii, *Quantum Electrodynamics*, 2nd ed. (Interscience, Wiley, New York, 1965).
[7] T. Suric, P.M. Bergstrom, Jr., K. Pisk, and R.H. Pratt, Phys. Rev. Lett. **67**, 189 (1991); P.M. Bergstrom, Jr., T. Suric, K. Pisk, and R.H. Pratt, Phys. Rev. A **48**, 1134 (1993).
[8] (a) M. Gavrila, Phys. Rev. A **6**, 1348 (1972), NR case with retardation; (b) **6**, 1360 (1972), NR dipole approximation.
[9] V. Florescu and M. Gavrila, Phys. Rev. A **14**, 211 (1976).
[10] W. Pauli, Helv. Phys. Acta **6**, 279 (1933).
[11] We note that this question is similar to that posed later by M. Gell-Mann, M.L. Goldberger, and W. Thirring, Phys. Rev. A **95**, 1612 (1954), in connection with dispersion-relations theory: does the ER limit of the forward Rayleigh scattering matrix element for arbitrary Z go over at $\omega\to\infty$, into that for scattering from a free electron (equal to the classical electron radius, r_0)? The answer, here too, was negative, contrary to what one had originally expected (see Ref. [9], and references therein).
[12] H. Casimir, Helv. Phys. Acta **6**, 287 (1933).
[13] (a) J. McEnnan and M. Gavrila, Phys. Rev. A **15**, 1537 (1977); (b) **15**, 1557 (1977).
[14] J.M. Jauch and F. Rohrlich, *The Theory of Electrons and Photons* (Springer, New York, 1976), Sec. 16.1.
[15] L. Rosenberg and F. Zhou, Phys. Rev. A **44**, 7283 (1991).

[16] R.H. Boyer, Phys. Rev. **117**, 475 (1960).
[17] B. Nagel, Ark Phys. **24**, 151 (1962).
[18] R.H. Pratt, Phys. Rev. **117**, 1017 (1960).
[19] V. Florescu and M. Gavrila, Radiat. Phys. Chem. **59**, 127 (2000).
[20] We recall that the infrared divergence of Compton scattering plays a central role in the calculation of the radiative corrections to the photoeffect, according to the regularization program of QED. The relativistic calculation was carried out to lowest order in αZ by J. McEnnan and M. Gavrila [13], and D.J. Botto and M. Gavrila, Phys. Rev. A **26**, 237 (1982).
[21] E. der Mateosian and M. McKeown, *Table of Gamma Rays Emitted by Radioactive Nuclei* BNL 605 (T-177), Physics and Mathematics (Brookhaven National Laboratory, Upton, NY, 1960).
[22] (a) V.N. Litvinenko *et al.*, Phys. Rev. Lett. **78**, 4569 (1997); (b) M. Hosaka *et al.*, Nucl. Instrum. Methods Phys. Res. A **393**, 525 (1997); (c) M.E. Couprie *et al.*, J. Phys. B **32**, 5657 (1999).
[23] *The Universe in Gamma Rays*, edited by V. Schönfelder (Springer, New York, 2001).
[24] See Ref. [6], Secs. 26.1 and 35. Our matrix element $M^{(C)}$ is related to the S-matrix element of the process by $S_{21} = -2\pi i(2\pi\alpha)(\kappa_1\kappa_2)^{-1/2}M^{(C)}\delta(E_0+\kappa_1-E_p-\kappa_2)$.
[25] That is, with asymptotic plane wave amplitude $(2\pi)^{-3/2}$.
[26] By integrating Eq. (9) over $d\Omega_2$ or $d\kappa_2$, singly differential cross sections are obtained, which are analogs of the Klein-Nishina cross sections differential with respect to $d\kappa_2$ or $d\Omega_2$, see Sec. 28.5 of Ref. [6].
[27] (a) L. Hostler, J. Math. Phys. **5**, 591 (1964); (b) **5**, 1235 (1964).
[28] See Ref. [27(a)], Sec. III. Our G differs from Hostler's K, i.e., $G=-K\beta$, but our G_I coincides with his [see his Eq. (3.9)].
[29] J. Schwinger, J. Math. Phys. **5**, 1606 (1964). The nonrelativistic Green's function G_0 which appears in Eq. (38) is related to that of Schwinger G_S, by $G_0=G_S/2$. We use the form of G_S given in Eq. (3.3′) of his paper.
[30] This is possible, however, as long as the matrix element thus calculated does not vanish for some value of its parameters, in which case the inclusion of the second term in Eq. (37) is required. This situation does actually happen at $\xi=0$, see Sec. V.
[31] For example, see Sommerfeld's book [4], Chap. VI, Sec. 4, Eq. (15b). Note that the $L_n(\rho)$ introduced there is defined by $L_n(\rho) \equiv {}_1F_1(-n,1;\rho)$.
[32] For $p\to\infty$, and at arbitrary momentum value $\mathbf{q}$, the second term in Eq. (37) gives a contribution of the same order as the first one. Only if $\mathbf{q}\equiv\mathbf{p}+\mathbf{a}$, where $\mathbf{a}$ is any constant vector, does Eq. (49) hold.
[33] Indeed, because of the convergence of the integral Eq. (40) with respect to the variables $\mathbf{p}_1,\mathbf{p}_2$, only a finite domain, say $|\mathbf{p}_1|<L$, $|\mathbf{p}_2|<L$, contributes to the integration. If κ_1 is sufficiently large with respect to L, we get the stated result.
[34] H.A. Bethe and E.E. Salpeter, *Quantum Mechanics of One-and Two-Electron Atoms* (Springer, New York, 1957).
[35] See A. Erdelyi *et al.*, *Higher Transcendental Functions* (McGraw-Hill, New York, 1953), Vol. I.
[36] M. Gavrila and A. Costescu, Phys. Rev. A **2**, 1752 (1970); **4**, 1688 (1971).
[37] No approximations have been made when passing from Eq. (74) to Eq. (76).
[38] It is worth noting that the integral over ρ can be carried out analytically, as described for *A*, *only* for the sum d_1+d_2 (as needed), and not for the separate terms d_1 and d_2.
[39] P. Appell and J. Kampé de Fériet, *Fonctions Hypergéometriques et Hypersphériques* (Gauthiers-Villars, Paris, 1926).
[40] F. Bell, J. Chem. Phys. **85**, 1 (1986).